Institutional Repository - Research Portal
Dépôt Institutionnel - Portail de la Recherche
researchportal.unamur.be
University of Namur

THESIS / THÈSE

MASTER IN CHEMISTRY PROFESSIONAL FOCUS

Synthesis of benzamidine-based low-molecular-weight inhibitors extending into the S3 pocket of FXIIa

BACQ, Marie

Award date:
2026

Awarding institution:
University of Namur

Link to publication

General rights
Copyright and moral rights for the publications made accessible in the public portal are retained by the authors and/or other copyright owners and it is a condition of accessing publications that users recognise and abide by the legal requirements associated with these rights.

- Users may download and print one copy of any publication from the public portal for the purpose of private study or research.
- You may not further distribute the material or use it for any profit-making activity or commercial gain
- You may freely distribute the URL identifying the publication in the public portal ?

Take down policy
If you believe that this document breaches copyright please contact us providing details, and we will remove access to the work immediately and investigate your claim.

Download date: 21. Aug. 2026

University of Namur

Faculty of Sciences

SYNTHESIS OF BENZAMIDINE-BASED LOW-MOLECULAR-WEIGHT INHIBITORS EXTENDING INTO THE S3 POCKET OF FXIIa

Master thesis submitted for the academic degree of

Master in Chemistry in "Chemistry of Living": Professional focus in Chemistry in Industry

Marie BACQ

January 2026

UNIVERSITY OF NAMUR
Faculty of Sciences
Education of the Department of Chemistry
Rue de Bruxelles 61 – 5000 NAMUR
Telephone: +32(0)81 72.54.44
E-mail: enseignement.chimie@unamur.be - www.unamur.be/sciences

Synthesis of benzamidine-based low-molecular-weight inhibitors extending into the S3 pocket of FXIIa

BACQ Marie

Abstract

Blood-contacting medical devices, such as catheters or stents, are widely used in clinical practice. However, their application is frequently associated with thromboembolic complications resulting from the activation of the coagulation enzyme FXII through the contact activation system. This requires anticoagulant treatment, but all currently used drugs inhibit downstream coagulation factors FXa or thrombin, which interfere with the coagulation process and cause a high risk of severe bleeding. Unlike other factors, FXIIa is not required for hemostasis, making it a promising therapeutic target for the development of safer inhibiting alternatives to common anticoagulants.

This work aims to provide new insights into the development of potent and selective FXIIa inhibitors by focusing on the design and synthesis of benzamidine-based small molecules. Benzamidine is known to be an S1-binding fragment for serine proteases and will be extended to the S3 pocket of FXIIa containing aromatic residues, through the grafting and testing of diverse S3-binding substituents to enhance affinity and selectivity for FXIIa.

The chosen approach relies on the synthesis of a common intermediate targeting the S1 pocket and the oxyanion hole, which serves as a basis for further structural elaboration. Key steps include a Pd-catalyzed cross-coupling reaction under Buchwald-type conditions, followed by a sensitive reduction step. This methodology constitutes a promising building block for the future development of FXIIa inhibitors.

Master Thesis in Chemical Sciences with a Professional Focus in Chemistry in Industry

January 2026

Promotor: S. Lanners

UNIVERSITE DE NAMUR
Faculté des Sciences
Secrétariat du Département de Chimie
Rue de Bruxelles 61 – 5000 NAMUR
Téléphone : +32(0)81 72.54.44
E-mail : enseignement.chimie@unamur.be - www.unamur.be/sciences

Synthèse d'inhibiteurs de bas poids moléculaire sur base de la benzamidine s'étendant dans la poche S3 de FXIIa

BACQ Marie

Résumé

Les dispositifs médicaux en contact avec le sang, tels que les cathéters ou les stents, sont largement utilisés en pratique clinique. Toutefois, leur utilisation est fréquemment associée à des complications thromboemboliques, résultant de l'activation de l'enzyme de coagulation FXII par le système d'activation par contact. Ces complications nécessitent un traitement anticoagulant, mais les médicaments actuellement utilisés inhibent les facteurs de coagulation en aval tels que FXa ou la thrombine, ce qui interfère avec le processus de coagulation et entraîne un risque élevé d'hémorragie sévère. Contrairement à d'autres facteurs, FXIIa n'est pas indispensable à l'hémostase, ce qui en fait une cible thérapeutique prometteuse pour le développement d'alternatives inhibitrices plus sûres aux anticoagulants courants.

Ce travail vise à apporter de nouvelles perspectives au développement d'inhibiteurs puissants et sélectifs de FXIIa en se concentrant sur la conception et la synthèse de petites molécules sur base de la benzamidine. La benzamidine est un fragment connu pour les protéases à sérine qui se lie dans la poche S1, et sera étendue à la poche S3 de FXIIa contenant des résidus aromatiques. Cette stratégie se base sur l'introduction et l'évaluation de divers substituants ciblant S3 afin d'améliorer l'affinité et la sélectivité vis-à-vis de FXIIa.

L'approche choisie repose sur la synthèse d'un intermédiaire commun ciblant la poche S1 et le trou oxyanionique, servant de base à une expansion ultérieure de ces fragments vers les autres poches. Les étapes clés comprennent une réaction de couplage catalysée par le palladium dans des conditions de type Buchwald, suivie d'une étape de réduction délicate. Cette méthodologie constitue une stratégie prometteuse pour le développement futur d'inhibiteurs de FXIIa.

Mémoire de Master en Sciences Chimiques à Finalité Spécialisée en Chimie d'entreprise

Janvier 2026

Promoteur : S. Lanners

ACKNOWLEDGEMENTS

C'est à la fin de ce travail que je rédige ces remerciements. Je me rends compte de tout le chemin ayant été parcouru durant cette année de mémoire, et plus généralement durant mes études. Je tiens d'abord à remercier tous les professeurs qui m'ont enseignée et accompagnée au cours de ces dernières années, et à qui je dois le développement considérable de mon goût pour la chimie.

Par ces remerciements, je pense à toutes les personnes qui ont contribué, de près ou de loin, à leur manière, à la réalisation de ce mémoire et à me soutenir pendant certains moments difficiles.

Je tiens à remercier particulièrement le Professeur Steve Lanners qui m'a permis d'intégrer son laboratoire, qui m'a guidée et aidée dans les impasses au travers de ses conseils toujours judicieux et de son savoir qui semble sans limite. Cela a été un réel plaisir d'avoir été son étudiante et d'avoir pu accumuler davantage de connaissances dans son domaine de prédilection qu'est la chimie organique. Je tiens aussi à adresser mes plus sincères remerciements à Amandine Traina, mon encadrante qui a su m'accompagner, me soutenir, et m'aider à avancer pas à pas, ensemble, pour mener à bien ce mémoire. Toujours bienveillante, disponible et prête à répondre à mes questions, ses conseils ont été indispensables à la réalisation de ce projet. Je lui suis profondément reconnaissante pour avoir contribué à ma formation de chimiste organicienne, pour sa patience, son écoute et son aide précieuse.

Je remercie également les collègues du COS, Loris, Pierre, Bastien, puis Alessia, Lison et Lionel arrivés plus tard, pour leur bonne humeur et leur humour très décalé, parfois déconcentrant. Vous avez contribué à une ambiance agréable et étiez toujours prêts à m'aider et à me conseiller. On ne s'ennuyait jamais avec vous, ça a été un plaisir d'avoir des discussions intéressantes et (de temps en temps) enrichissantes avec vous.

Mes remerciements se tournent ensuite vers mes camarades de classe et amis, le fameux groupe IKEA avec Florian, Florina (les Flo^2), Nicolas, Ethaniel, Bastien et Thomas, mais aussi Savannah. Merci pour nos délires, nos soirées, nos sorties à l'Irish qui m'ont toujours fait penser à autre chose quand j'en avais besoin, mais surtout pour vos conseils, vos encouragements (réciproques), votre présence et votre soutien. Je pense aussi à Emilie qui m'a énormément soutenue et qui croyait toujours en moi malgré les moments difficiles. Mes copines de secondaire Aurélie, Sara et Sophia ont aussi contribué, malheureusement pas assez souvent, à passer des moments agréables sans penser aux études et à pouvoir m'épanouir en dehors de l'université. Je pense aussi à toutes ces personnes que j'ai rencontré lors d'activités extra-universitaires comme la Revue Sciences ou le kàp Une Fois Namur, je ne pourrais pas tous vous citer mais je vous

remercie grandement de m'avoir permis de vivre de chouettes moments à côté des études. Votre présence à chacun.e m'a permis de me pousser vers la fin de ces études et de m'apporter une bouffée d'air frais dans cet environnement universitaire parfois exigeant.

Je tiens aussi à exprimer toute ma gratitude à ma famille, mon papa qui ne comprenait pas grand-chose à ce que je faisais mais qui me motivait tout de même, et en particulier ma maman pour son soutien inconditionnel, sa confiance en moi et ses encouragements constants tout au long de ces quelques dernières années. Merci à mes parents d'avoir toujours été là pour moi et de m'avoir écoutée me plaindre, votre bienveillance a permis de mener ce parcours du combattant que sont les études à bien. Une petite pensée à mon frère Simon pour avoir répondu à mes questions d'ordre médical sur ce mémoire et pour s'être intéressé à mon projet, et à Mathieu pour avoir exprimé, à ta manière bien particulière, ton soutien et tes encouragements pour persévérer dans ce projet malgré les difficultés. Je pense aussi à Nicolle qui a toujours su m'encourager et me soutenir au cours de ces études, et ma famille de Pologne, qui, malgré la distance, me soutient de tout son cœur et qui est (je l'espère) fière de moi.

Je remercie sincèrement Nathan, qui a aussi toujours été là pour moi, qui a toujours su me soutenir et me réconforter dans les moments de doutes et de difficultés. Ce mémoire et la fin de mes études n'auraient probablement pas été possibles sans lui. Je pense à tous les moments où tu m'as accompagnée, encouragée, et où tu m'as permis de me changer les idées. Ce n'était pas toujours évident, mais tu as toujours su faire de ton mieux pour que je me sente la plus épanouie possible. Merci infiniment pour ta présence, ton aide et tes conseils pour certains travaux. Je remercie aussi sa famille, qui m'a constamment envoyé des petites attentions, et encouragée à chaque fois que je les voyais.

Enfin, je souhaite avoir une pensée toute particulière pour mes grands-parents partis il y a quelques années, qui n'ont malheureusement pas pu voir l'aboutissement de mes études. Je ne cesse de penser à eux, à leur soutien et leurs encouragements de là-haut, et à combien ils auraient été fiers de me voir persévérer et arriver au bout de ces études. Babciu i dziadku, tęsknie za wami. Je pense aussi à Jacques parti trop tôt, qui aurait été fier de voir la chimiste que je suis devenue.

TABLE OF CONTENTS

LIST OF ABBREVIATIONS

AMINO ACIDS

Arg	Arginine
Asn	Asparagine
Asp	Aspartate
Gly	Glycine
His	Histidine
Leu	Leucine
Phe	Phenylalanine
Pro	Proline
Ser	Serine
Trp	Tryptophan
Tyr	Tyrosine
Val	Valine

ANALYSES

aPTT	Activated partial thromboplastin time
ESI	Electrospray ionization
FT-IR	Fourier transform infrared spectroscopy
HRMS	High resolution mass spectrometry
IC_{50}	Half maximal inhibitory concentration
M_p	Melting point
NMR	Nuclear magnetic resonance
ppm	Parts per million
PT	Prothrombin time
R_f	Retention factor
TLC	Thin layer chromatography
TOF	Time of flight
UV	Ultraviolet
XRD	X-ray diffraction

CHEMICAL TERMS

Ac	Acetyl
Cy	Cyclohexane

dba	Dibenzylideneacetone
DIBAL-H	Diisobutylaluminum hydride
DMF	Dimethylformamide
eq	Equivalent
NMP	1-methyl-2-pyrrolidinone
TBDMSCl	*tert*-butyldimethylsilyl chloride
TBME	*tert*-butyl methyl ether
*t*Bu	*tert*-butyl
THF	Tetrahydrofuran

COAGULATION FACTORS

FV	Coagulation factor V
FVa	Activated coagulation factor V
FVII	Coagulation factor VII
FVIIa	Activated coagulation factor VII
FVIII	Coagulation factor VIII
FVIIIa	Activated coagulation factor VIII
FIX	Coagulation factor IX
FIXa	Activated coagulation factor IX
FX	Coagulation factor X
FXa	Activated coagulation factor X
FXI	Coagulation factor XI
FXIa	Activated coagulation factor XI
FXII	Coagulation factor XII
FXIIa	Activated coagulation factor XII
FXIIf	Coagulation factor XII fragment
FXIII	Coagulation factor XIII
FXIIIa	Activated coagulation factor XIII
PTHR	Prothrombin
TF	Tissue factor
THR	Thrombin

OTHERS

ASO	Antisense oligonucleotide
BCMD	Blood-contacting medical device
BK	Bradykinin

C1-INH	C1 esterase inhibitor
CAS	Contact activation system
CD	Catalytic domain
CTI	Corn trypsin inhibitor
DIC	Disseminated intravascular coagulation
DOAC	Direct oral anticoagulant
DVT	Deep vein thrombosis
ECMO	Extracorporeal membrane oxygenation
EGF	Epidermal growth factor
FnI	Fibronectin type I domain
FnII	Fibronectin type II domain
HAE	Hereditary angioedema
HK	High-molecular-weight kininogen
Ir-CPI	*Ixodes ricinus* contact phase inhibitor
kDa	Kilo Dalton
LMWH	Low-molecular-weight heparin
M	Molar
mRNA	Messenger ribonucleic acid
PCK	D-Pro-Phe-Arg-chloromethyl ketone
PDB	Protein data base
PE	Pulmonary embolism
PK	Plasma kallikrein
PolyP	Polyphosphate
PPK	Plasma prekallikrein
PRR	Proline rich region
RISC	Ribonucleic acid-induced silencing complex
siRNA	Small interfering ribonucleic acid
UFH	Unfractionated heparin
VKA	Vitamin K antagonists
VKORC1	Vitamin K epoxide reductase complex subunit 1
VTE	Venous thromboembolism
VWF	von Willebrand factor

INTRODUCTION

1. HEMOSTASIS AND COAGULATION CASCADE

Whenever an injury occurs, the body must quickly restore vascular integrity. Once the blood vessel is damaged, vasoconstriction occurs immediately as a reflex to limit blood loss.[1] Injuries also trigger hemostasis, the physiological process that results in the formation of a blood clot to prevent bleeding. Several processes constitute hemostasis, namely primary and secondary hemostasis, ending with fibrinolysis.[2]

The innermost layer of a blood vessel, the endothelium, is lined with endothelial cells: its purpose is to maintain the blood that is directly in contact with it in a fluid state.[1,3] In the event of a blood vessel rupture, primary hemostasis begins: components of the subendothelial matrix, such as collagen, fibronectin and especially von Willebrand factor (VWF), are released and become exposed to the blood. These components adhere to platelets to activate them, which results in platelet aggregation and forms a blood clot (Figure 1).[2,4]

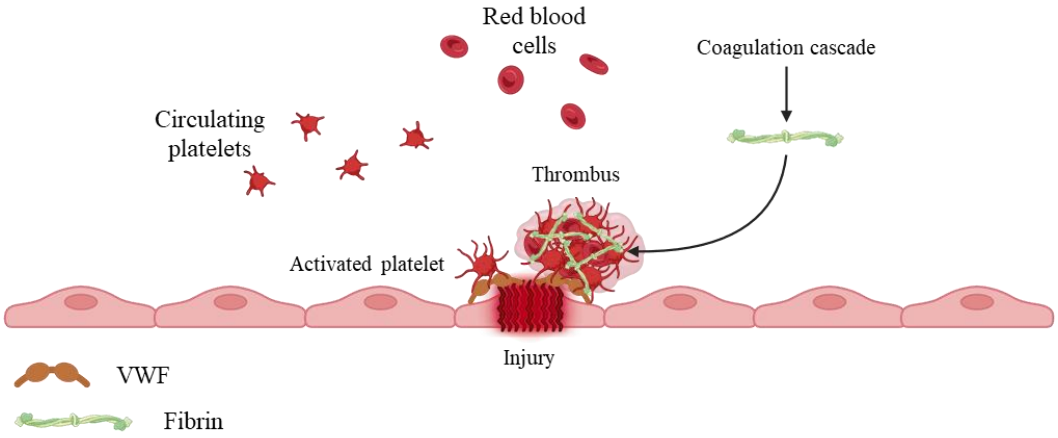

Figure 1. Schematic representation of the hemostasis process. After an injury, VWFs are exposed to circulating blood containing platelets which become activated. Accumulated platelets, red blood cells, and generated fibrin clot by coagulation factors form a thrombus. Figure created with BioRender.

When the injury occurs, the coagulation cascade, also called secondary hemostasis, is initiated simultaneously with primary hemostasis, as these two phases are linked to each other and intertwined. Secondary hemostasis will ultimately form an insoluble cross-linked fibrin polymer that binds the platelets together and stabilizes the generated blood clot at the site of the injury (Figure 1).[2] This cascade model has been first described by two different teams around 1964: R. G. MacFarlane[5] and O. D. Ratnoff in collaboration with E. W. Davie.[6] This process involves coagulation factors, zymogens, which are inactive forms of serine proteases, that cleave and activate each other in a cascade model, hence the name. Figure 2 shows an overview of this process where the contact activation system (CAS), the intrinsic, extrinsic and common pathways are represented.

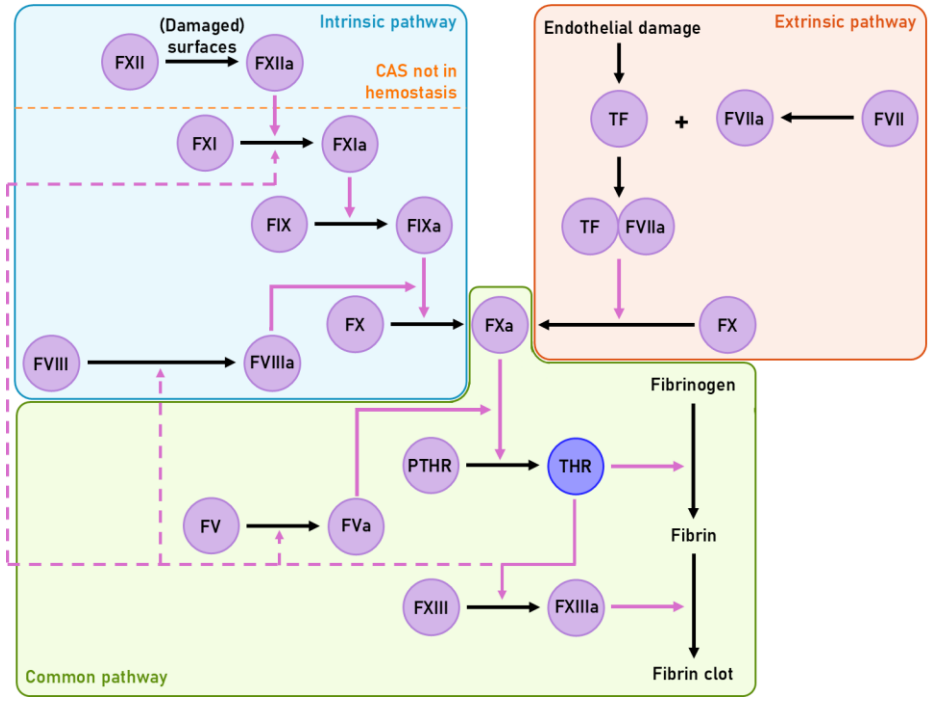

Figure 2. The coagulation cascade: the intrinsic pathway is initiated by FXIIa, and the extrinsic pathway is initiated by the TF-FVIIa complex. The arrows in black represent the reactions involved, and the arrows in pink represent the activation of these reactions. CAS = contact activation system; TF = tissue factor; PTHR = FII = prothrombin; THR = thrombin. Adapted from refs. 2,3,7.

Both the intrinsic and extrinsic pathways lead to a common pathway and to the activation of FX. Injuries to the vascular endothelium trigger the extrinsic pathway, releasing tissue factor (TF) which is a cofactor of FVIIa that becomes exposed to the blood. The formed TF-FVIIa complex activates FX, that eventually converts prothrombin (PTHR) into thrombin (THR). Thrombin formation is initiated by the extrinsic pathway, and its propagation is intensified by a feedback loop *via* the intrinsic and common pathway (dotted arrows in Figure 2). Thrombin plays several roles: it initiates the intrinsic pathway by the activation of FXI, which is followed by the activation of FIX by FXIa, and the activation of FX by FIXa and its cofactor FVIIIa. It also activates the conversion of fibrinogen into fibrin, which binds the generated platelet plug by the formation of a polymer of fibrin with the help of FXIIIa.[2,3,7]

The intrinsic pathway can also be initiated *via* the CAS with the activation of FXII by artificial or negatively charged natural surfaces, which will be further detailed in Section 3.3. However, the CAS is dispensable to hemostasis to generate a blood clot, as the coagulation cascade can be initiated through other pathways, namely the extrinsic pathway, and can be propagated through thrombin activation.

As for wound healing and blood vessel regeneration, fibrinolysis consists in dissolving the generated blood clot, preventing the thrombi to circulate in healthy blood vessels. Plasmin, one of the implied enzymes, functions to break down fibrin, leading to the degradation of the clot.[2]

2. THROMBOSIS

2.1. Thrombosis and thromboembolism

Thromboembolic complications including strokes, myocardial infarctions, or pulmonary embolism (PE) represent a major global health concern: these events are the leading cause of mortality, with millions of deaths globally that accounted for one in four deaths in 2010, and still do to this day.[8] Not only is death a possible unfortunate outcome, but patients who survive venous thromboembolism (VTE) might have an increased risk of developing ulcers and severe post thrombotic syndrome, a chronic disorder that diminishes the quality of life by reducing the ability to walk and work. As for patients surviving PE, some individuals may experience chronic thromboembolic pulmonary hypertension, which causes respiratory or cardiac disorders varying in severity. VTEs and PEs could lead to long-term impairments that go beyond "simple" thrombosis. In addition to these possible disorders, psychological consequences such as stress and anxiety about the uncertainty of recurrence could occur.[9] To put it briefly, the prevalence of thromboembolic events make thrombosis a crucial focus of clinical and therapeutic research.

Thrombosis refers to the pathological and uncontrolled formation of a blood clot, called a thrombus, which obstructs blood flow in a blood vessel as a consequence of dysregulated hemostasis.[3,7,10,11] In some cases, this thrombus can detach partially or completely, becoming what is commonly referred to as an embolus, which causes thromboembolism whenever the blood flow is interrupted by an occluded blood vessel. Both processes can occur in arteries or veins and generally lead to different outcomes: arterial thromboses are more likely to cause myocardial infarction or stroke, while venous thromboses cause deep vein thrombosis (DVT) or PE. Thrombosis can also occur in the chambers of the heart, but will not be described here.[3] In the context of this thesis, the cause of thrombosis that is the most relevant is BCMD-induced thrombosis (Section 2.1.3).

2.1.1. Arterial thrombosis

Arterial thrombosis occurs due to endothelial injury, mainly initiated by atherosclerosis, as shown in Figure 3. Atherosclerosis is a condition consisting in the accumulation of fats such as lipoproteins, lipids, and especially cholesterol, as well as cellular debris from macrophages. These build-ups form atheroma, also called atherosclerotic plaques. As the atheroma grows, it progressively restricts the space in which the blood flows and narrows the blood vessel. Damage to the blood vessel occurs either by cholesterol crystals formed in the plaques possibly rupturing them, or by the high blood flow that could cause erosion of the vessel wall. Components of the

subendothelial matrix (collagen, fibronectin, VWF) become exposed, which initiate the coagulation process by the activation and adhesion of platelets, as described in Section 1. The generated blood clot, formed around the ruptured atherosclerotic plaques, is enriched in aggregated platelets due to the high blood flow of arteries, and could obstruct the blood vessel due to the narrowing of the lumen, leading to thrombotic events.[10,12,13]

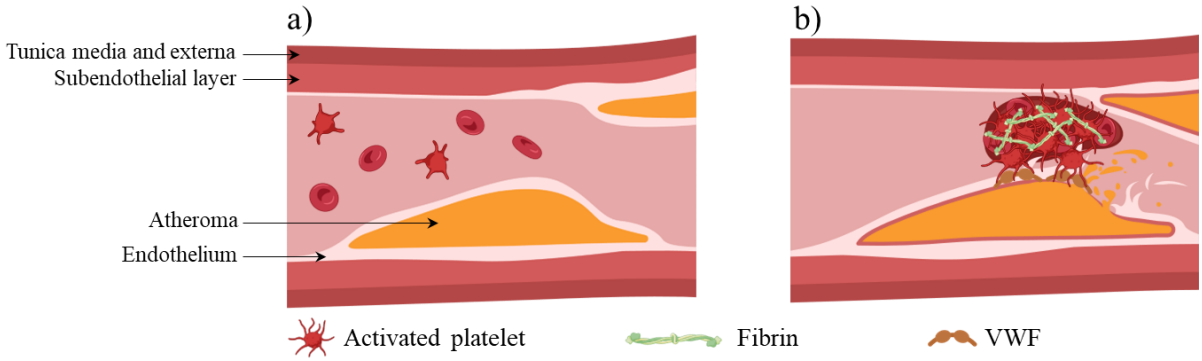

Figure 3. a) Atherosclerotic plaque between the endothelium and the subendothelial matrix in an artery. b) Endothelium rupture leads to exposition of VWF to blood, leading to platelet activation and aggregation. The coagulation cascade is initiated by the TF-FVIIa complex to form a fibrin clot stabilizing the platelet-rich thrombus. Figure created with BioRender.

2.1.2. Venous thrombosis

Venous thromboembolism is a condition where a thrombus forms in the veins, and most commonly occurs in the deep veins of the lower limbs, which is known as DVT. The blood clot can also embolize and travel to the lungs, which causes PE. The current understanding of venous thrombosis is based on Virchow's triad, a concept first proposed over 150 years ago by Rudolf Virchow, which identifies three primary factors contributing to the formation of venous thrombi: blood stasis, vascular injury and hypercoagulability.[3,7,14]

Unlike arteries, blood flow is significantly lower in veins. As shown on Figure 4a-b, to ensure unidirectional movement of blood and to prevent reflux, veins contain valves, of which the amount can vary among individuals. However, blood flow patterns can be irregular: blood stasis can lead to the accumulation of procoagulant proteases as well as low oxygen levels (called hypoxia), which make the valve sinus particularly prone to thrombosis. This lack of oxygen is a critical factor, as hypoxia or inflammation can activate the vascular endothelium: activated endothelial cells express VWF which can bind to platelets, and selectins that can bind to leukocytes and microvesicles (Figure 4c). Bound leukocytes become activated, and together with microvesicles, can express TF, which initiates the coagulation cascade *via* the extrinsic pathway (TF and platelet accumulation). The resulting vein blood clot is rich in fibrin and red blood cells (Figure 4d). This thrombus prevents the valve from opening, which blocks blood flow.[10,15]

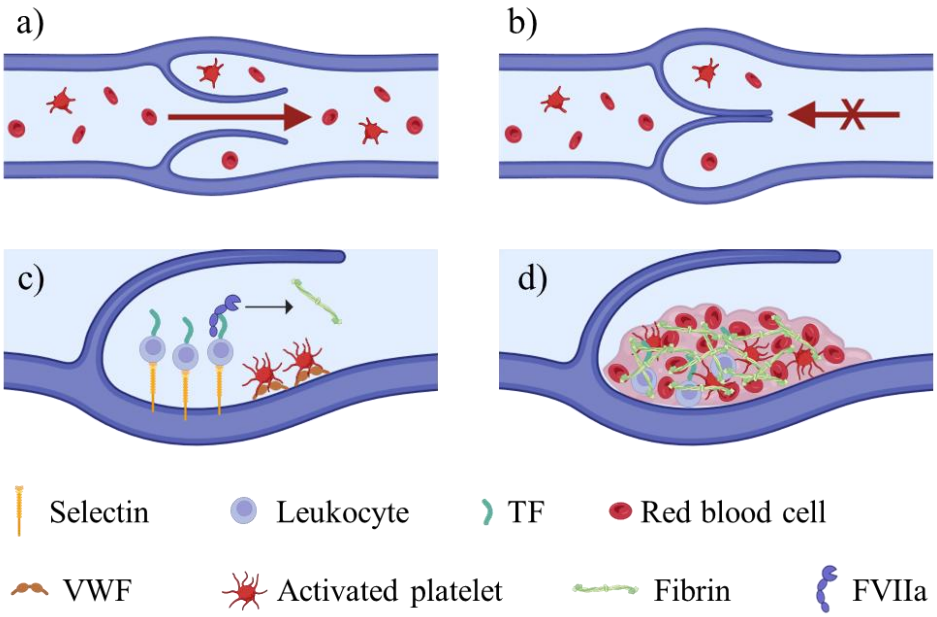

Figure 4. a) Unidirectional flow of blood in a vein. b) Blood prevented from flowing in the wrong direction in a vein. c) Activated endothelial cells express VWF binding to platelets, and selectins binding to leukocytes that become activated and express TF. The coagulation cascade is initiated by TF and FVIIa to form fibrin. d) The thrombus prevents the vein valve from opening. Figure created with BioRender.

Acquired risk factors for venous thrombosis and thromboembolism include genetic risk factors such as FV Leiden mutation, but also cancer, surgery, obesity, immobilization, and pregnancy that can cause an hypercoagulable state.[2,3,7,15]

2.1.3. BCMD-induced thrombosis

Blood-contacting medical devices (BCMD) such as vascular grafts, stents, catheters, dialysis circuits or heart valves play a crucial role in medical practice, mainly to treat cardiovascular diseases. However, their application is often associated with thromboembolic complications, where blood clots can cause device failure, resulting in severe thrombotic events.[16]

Plasma proteins tend to adsorb rapidly on the device's surface, which promotes clotting through a series of interconnected processes. The accumulation of fibrinogen, fibronectin and VWF that deposit on these artificial surfaces can trigger platelet activation and aggregation as described in Section 1. Adsorbed fibrinogen is quickly replaced with components of the contact system: FXII, high molecular weight kininogen (HK), plasma prekallikrein (PPK), and FXI. FXII autoactivates on the medical device's surface, leading to FXIIa that can initiate the intrinsic pathway of the coagulation cascade by the activation of FXI which is in close proximity. Moreover, FXIIa can also cleave PPK into plasma kallikrein (PK) with the help of HK, resulting in a positive feedback loop generating more FXIIa. This is the CAS, which will be further described in Section 3.3.[16]

To prevent BCMD-induced thrombosis, efforts have focused on rendering artificial surfaces less thrombogenic and/or administrating antiplatelet drugs or anticoagulants. Additionally, surface modifications to resist adsorption of plasma proteins could be an interesting alternative.[16]

2.2. Anticoagulants

Thrombosis can be prevented with three types of drugs: antiplatelet drugs, anticoagulants and fibrinolytic agents.[7] Since arterial thrombi are enriched in platelets, arterial thrombosis is usually prevented with antiplatelet drugs, while venous thromboembolism and BCMD-induced thrombosis are prevented mainly by anticoagulant treatments.[17] Anticoagulants target enzymes of the coagulation cascade.

Unfractionated heparins (UFHs), also called heparins, are sulfated polysaccharides isolated from mammalian tissues, especially porcine intestinal mucosa.[7] UFH indirectly inhibits the coagulation cascade by activating antithrombin, a protein acting as a suicide thrombin and FXa inhibitor, *via* binding with a pentasaccharide sequence found on heparin. A conformational change is induced on antithrombin after binding with heparin, which makes antithrombin more readily accessible to its targets and enhances the rate at which antithrombin inhibits FXa.[7] UFHs are parenterally administered, intravenously or subcutaneously,[7,17] but present a limited bioavailability: heparin binds to the endothelium and to plasma proteins other than antithrombin, which causes a short half-life at low doses (around 1 hour), and reduces its anticoagulant activity.[7] The anticoagulant response is thus unpredictable depending on the blood composition of individuals, requiring patient close monitoring.[7,17] The most common side effect associated with UFH is bleeding, where the risk rises as the administered dose increases, but thrombocytopenia and osteoporosis are other possible complications.[7,17] Thrombocytopenia is a condition caused by low platelet counts, associated with an increased risk of thrombosis.[7,18] Heparin-induced osteoporosis is a disorder involving bone weakening and reduction in bone density, which can be caused by therapeutic treatment with heparin for over a month.[7] A general structure of a disaccharide of heparins can be found in Figure 5.

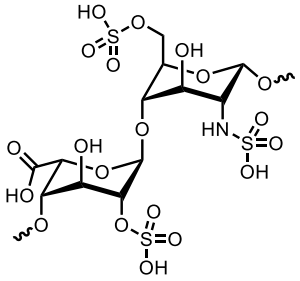

Figure 5. Common disaccharide unit found in heparins.

Low-Molecular-Weight Heparins (LMWHs) are smaller fragments of UFHs, usually a third in weight, obtained by enzymatic or chemical depolymerization.[7,17] The mechanism of action of LMWHs is fundamentally similar to UFHs: LMWHs are indirect anticoagulants through binding with and activation of antithrombin. However, since LMWH polysaccharide chains are shorter, they cannot bridge thrombin to antithrombin, inhibiting preferentially FXa.[7] LMWHs (for example, enoxaparin) are also parenterally administered, especially subcutaneously, and have a half-life of about 4 hours: they can be given once or twice daily.[7] They display an increased bioavailability of about 90% compared to UFHs, making them less prone to bind with other UFH-binding targets, which results in a more predictable anticoagulant response and does not require monitoring. Risk of bleeding and developing thrombocytopenia or osteoporosis is lower with LMWHs than with UFHs.[7,17] Due to the decrease of the intensity of undesired side effects, LMWHs have now replaced UFHs for most thrombotic indications.[17]

Fondaparinux is a synthetic analogue of the antithrombin-binding pentasaccharide sequence found in heparins.[7,17] Similarly to LMWHs, binding to antithrombin results in selective inhibition of FXa, since this molecule is too short to bridge thrombin to antithrombin. It distinguishes itself from heparins through its complete bioavailability following subcutaneous injection and does not bind at all to other UFH-binding targets. With a half-life of 17 hours, it allows for one daily dosing. While bleeding remains the primary side effect, fondaparinux does not induce thrombocytopenia.[7,17]

Direct thrombin inhibitors, such as argatroban and bivalirudin, bind directly to the active site of thrombin.[7] Argatroban (Figure 6) is a synthetic derivative of L-arginine used to treat patients with heparin-induced thrombocytopenia.[7,17] It is administered intravenously and has a half-life of about 45 minutes.[7] Bivalirudin, a synthetic 20-amino-acid peptide analogue of hirudin (originally isolated from leeches), acts as a divalent thrombin inhibitor.[7,17] Also administered parenterally, it has the shortest half-life of about 25 minutes and is licensed as an alternative to heparin for percutaneous coronary intervention, as well as patients affected by thrombocytopenia.[7]

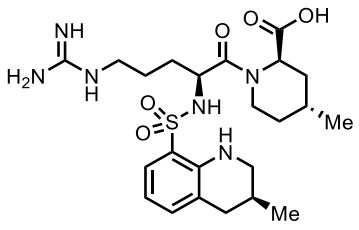

Figure 6. Structure of argatroban.

The synthesis of PTHR, FVII, FIX and FX is vitamin K-dependent through a vitamin K epoxide reductase complex subunit 1 (VKORC1), an enzyme involved in vitamin K recycling.[19] Vitamin K serves as a cofactor to catalyze γ-carboxylation, a post-translational modification of vitamin K-dependent proteins. Vitamin K antagonists (VKAs) are VKORC1 inhibitors, preventing vitamin K recycling and the γ-carboxylation of coagulation zymogens to be functional.[19] Warfarin (Figure 7), the most prescribed VKA in North America, is a synthetic molecule derived from coumarin. Although its oral administration appears convenient, the anticoagulant effect of warfarin is delayed to about 3 to 7 days until the elimination of already synthesized coagulation factors, thus needing other rapidly-acting treatments such as heparins.[7,17] Furthermore, the anticoagulant response varies from one individual to another depending on genetic, dietary and drug-drug factors.[7,17] A rigorous and frequent monitoring is required to adjust the dosage of warfarin.[17] Besides a hemorrhagic risk, warfarin could present other undesired side effects such as skin necrosis (which is rare) and fetal abnormalities, preventing warfarin intake during pregnancy.[7]

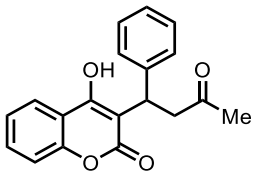

Figure 7. Structure of warfarin.

VKAs such as warfarin have been the only available oral anticoagulants for many years,[7] up until the recent discovery and approval of direct oral anticoagulants (DOACs) in the 2010s.[20] DOACs have become attractive alternatives with more effective, safe, and convenient treatment options to prevent thromboembolic complications.[20] These anticoagulants are small synthetic molecules and reversible inhibitors binding selectively to the active site of their target: examples of DOACs include dabigatran which directly inhibits thrombin, but also rivaroxaban, apixaban, and edoxaban, which inhibit FXa.[7,17,20] DOACs are administered orally with half-lives ranging from 5 to 17 hours, allowing once or twice daily administration.[7,17] These anticoagulants represent a significant improvement over VKAs due to their rapid absorption, their direct inhibition of coagulation factors, and fewer interactions with diet and other drugs. They are thus administered in fixed doses without the need for intense monitoring, as their anticoagulant response is more predictable.[7,17] The main risk of DOACs still remains bleeding: compared to warfarin, they are associated with less intracranial hemorrhage, but with more gastrointestinal bleeding. Moreover, DOACs are contraindicated in pregnancy.[7] Commonly used DOACs are represented in Figure 8.

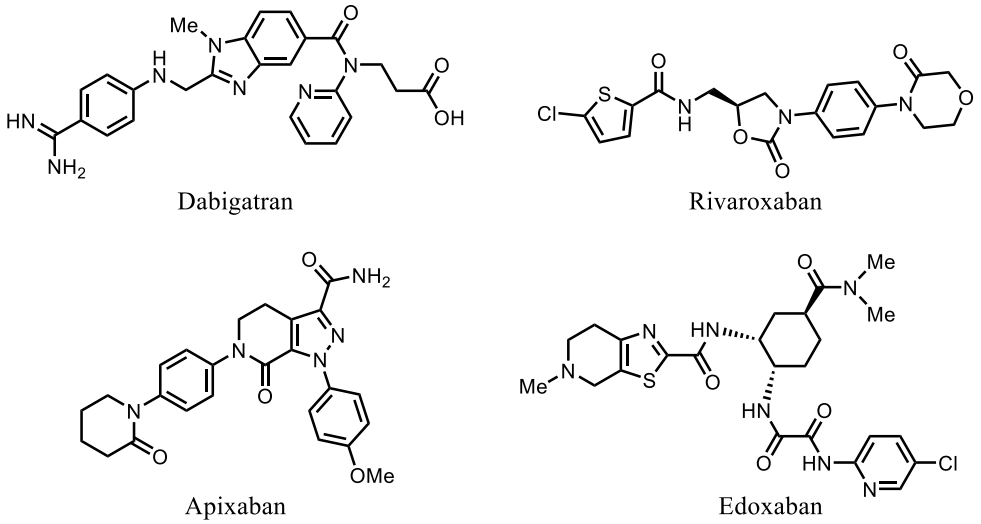

Figure 8. Structures of some DOACs.

Current anticoagulants, such as heparins, vitamin K antagonists, and DOACs, are effective for preventing thromboembolic complications, but come with significant constraints including issues with maneuverability and an associated hemorrhagic risk.[17] Their use is further limited by short half-lives, the need for mandatory patient monitoring, and other possible serious side effects. These drawbacks are particularly problematic for patients dependent on BCMD, as contact with artificial surfaces activates FXII, leading to a high risk of thrombosis. Alternatives therapies to these usual anticoagulants to prevent BCMD-induced thrombosis while maintaining the coagulation cascade need to be researched. As will be described in the following sections, FXII appears as a promising solution to prevent thrombosis without disrupting hemostasis.

3. FACTOR XII (FXII)

3.1. Background

FXII, also called Hageman factor, was first discovered in 1955, thanks to the work of O. D. Ratnoff, J. E. Colopy and colleagues[21] who described a surprising and apparently abnormal case: a patient named John Hageman, whose blood clotting time in glass test tubes turned out to be much slower than a reference sample, yet who did not encounter any bleeding tendency. His blood lacked a plasma fraction, later identified as an enzyme named after him, and the associated deficiency the Hageman trait. The first group to purify Hageman factor was supervised by O. D. Ratnoff and E. Davie, which they renamed factor XII (FXII).[22] E. Davie and O. D. Ratnoff, the pioneers of the waterfall coagulation model as described in Section 1, worked in collaboration to prove that this deficient fraction was a serine protease involved in the coagulation cascade. They discovered that the absence of FXII prevents the activation of FXI into FXIa which, in turn, activates FIX to engage the rest of the coagulation cascade *via* the intrinsic pathway.[23]

These observations were the basis for their hypothesis on the initiation of blood coagulation by contact activation.[24]

Interest in FXII has only grown throughout the years, as shown by the significant number of papers published in the literature since the 1970s.[24–28] These papers range from its role in the coagulation cascade and its implication in the CAS, to its amino acid sequence and structure further developed in the 1980s.[29] More recently, in the 2000s, another series of studies has focused, not on FXII itself, but rather on its therapeutic role.[30]

3.2. Structure

Coagulation FXII is a serine protease composed of 596 residues (~ 80 kDa) circulating in the bloodstream as an inactive zymogen that can be cleaved into its activated form FXIIa.[30] FXII can be categorized as a glycoprotein which is secreted by the liver, and has a weak proteolytic activity.[29,30] This enzyme is composed of a heavy chain (353 residues from N-terminal) and light chain (243 residues to C-terminal) bound together by a disulfide bond. As shown in Figure 9, the heavy chain contains mainly recognition domains: two fibronectin domains type II (FnII) and I (FnI), two epidermal growth factor-like domains (EGF1 and EGF2), a kringle domain and a proline-rich region (PRR).[3,29] The heavy chain can bind to negatively charged surfaces, while the light chain represents the trypsin-like catalytic domain (CD) including the catalytic triad that contains a serine (Ser195), an histidine (His57), and an aspartate (Asp102).

α-FXIIa, called FXIIa in this work, is produced by the cleavage between Arg353 and Val354, yielding a two-chain enzyme bound together by the disulfide bond. This cleavage induces a conformational change of FXIIa, which makes it activated and ready to participate in the CAS. Another cleavage can occur from FXIIa between Arg334-Asn335 and Arg343-Leu344 to discard a major part of the heavy chain: this fragment is called β-FXIIa or FXIIf and is also held by the disulfide bond.[29–31]

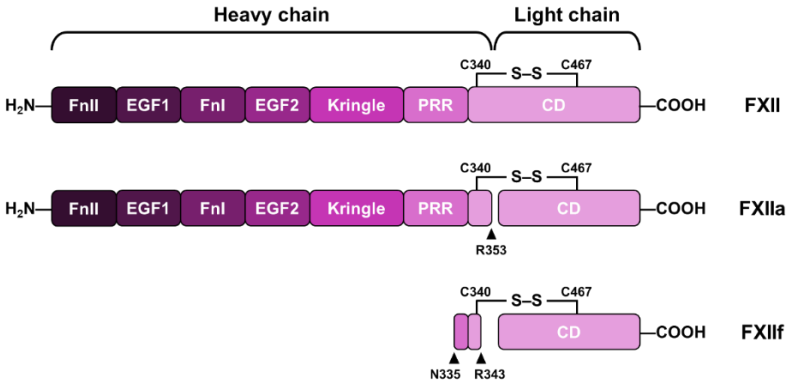

Figure 9. Structure and domains of FXII, FXIIa and FXIIf.

Human FXIIf has been successfully co-crystallized with benzamidine: Figure 10 highlights the 3D structure of FXIIf, the different pockets, as well as key residues (PDB ID: 6B74).[32]

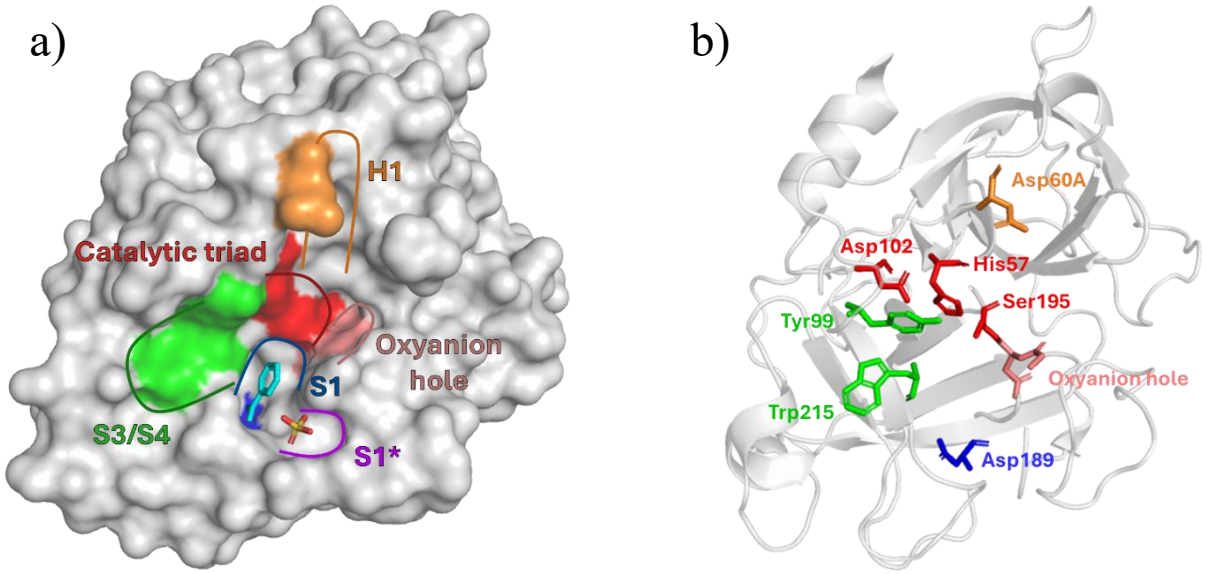

Figure 10. a) Molecular surface representation of human FXIIf co-crystallized with benzamidine and the different highlighted pockets. b) Residues of FXIIf numbered according to the chymotrypsin numbering system (PDB ID: 6B74).[32]

The catalytic triad is made up of His57, Asp102 and Ser195, following the chymotrypsin numbering system. The oxyanion hole stabilizes the negative charge of the tetrahedral intermediate by H-bonding with the backbone amidic hydrogens of Ser195, Asp194 and Gly193.

The main pocket S1 is characterized by Asp189 at its bottom, a negatively charged residue that can interact with positively charged ones, especially Arg of other enzymes to induce their cleavage. The S3/S4 pocket, later called S3 in this work, is an aromatic pocket containing Tyr99 and Trp215. The H1 hydrophobic pocket contains aliphatic residues such as Leu33, Leu54, Leu59, and Leu106. Asp60A appears next to this pocket as a protuberance.[32]

A subpocket near S1, which was named S1* by our group, that contains a sulfate ion in the crystal structure, has also been observed.[32] It appears as a specificity of FXIIa, and could therefore be an interesting target to increase selectivity towards FXIIa.

3.3. The CAS and activating surfaces

The CAS is an ensemble of interconnected processes, a pivot between blood coagulation and inflammatory response, where the main components involved are enzymes FXII, FXI, PPK, and non-enzymatic cofactor HK.[31,33–35]

As described briefly in Section 2.1.3., the CAS (which is represented in Figure 11), and especially the kallikrein-kinin system, is initiated whenever FXII is adsorbed on and binds to negatively charged or artificial surfaces: FXII undergoes conformational changes to autoactivate into FXIIa and to develop a weak proteolytic activity. FXIIa cleaves PPK into PK with the help of HK: FXII then becomes susceptible to cleavage by PK and FXIIa itself, resulting in a positive feedback loop producing more FXIIa. Furthermore, activated PK can cleave the precursor HK into bradykinin (BK), a small peptide responsible for increased vascular permeability and vasodilation. HK circulates as a complex with either FXI or PPK and acts as a scaffold to allow the enzymes to bind to these negatively charged or artificial surfaces.[31,33–35]

Blood coagulation can also be initiated *via* the CAS, as stated in Section 1. Once enough FXIIa is formed through the feedback loop involving PK, it can cleave FXI into FXIa and initiate the intrinsic pathway of the coagulation cascade.[31,34,35]

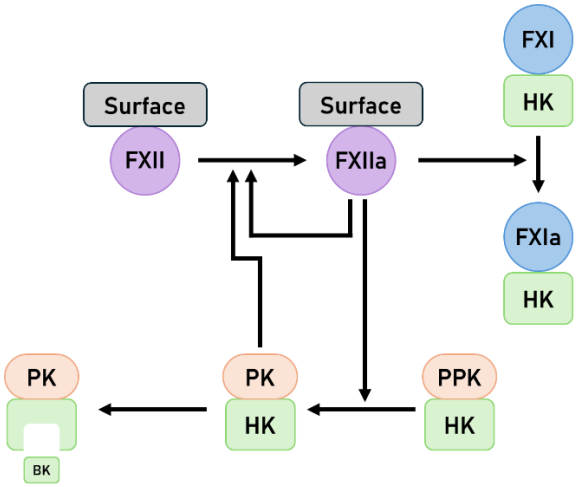

Figure 11. Overview of the CAS.

The nature of activating surfaces is diverse, which makes the classification complicated, as the requirements for being an activating surface are not well understood.[34] Examples of natural surfaces or compounds *in vivo* include polyphosphates (PolyPs) generated by platelets during blood coagulation, misfolded protein aggregates, collagen, nucleic acids, peptidoglycans, lipopolysaccharides, etc.[36,37] Some nonphysiological compounds used *in vitro* for the activated partial thromboplastin time (aPTT)[1] assays also initiate the contact pathway, such as kaolin, glass, silica, ellagic acid or sulfated polysaccharides (dextran sulfate, oversulfated chondroitin sulfate, etc.).[31,34–37] The terminology "negatively charged surfaces" is used because some of these compounds including PolyPs, kaolin, glass, ellagic acid (ellagate anion), among others, are

[1] The aPTT assay evaluates the time required for blood coagulation to occur via the intrinsic pathway.

known to be negatively charged activators. BCMD however, can be made of several materials, especially metals, polymers, ceramics, and composites, acting as artificial activating surfaces. Frequently used materials include titanium alloys, stainless steel, polyurethanes, polytetrafluoroethylene, polyethylene terephthalate, polyvinylchloride or polypropylene.[34,38] Despite these polymers being globally neutral, blood proteins and cells can still accumulate and adsorb at the BCMD surface, since blood is constantly flowing.[38] As this protein adsorption is favored by electrostatic and hydrophobic interactions between the adsorbed protein and the artificial surface, the coagulation cascade can be initiated by the CAS through protein accumulation, not involved in the CAS and circulating in the blood (particularly fibrinogen, fibronectin, and VWF).[16]

3.4. Disorders involving FXII

FXIIa is a central component of the CAS: excessive activation of this contact pathway can be involved in various diseases. In these contexts, FXIIa acts as an amplifier of the inflammatory response and blood coagulation, proving that CAS plays a key role in these pathologies.

3.4.1. Hereditary angioedema

Hereditary angioedema (HAE) is an orphan, genetic life-threatening tissue disorder characterized by recurrent episodes of acute swelling affecting the skin, larynx, oropharynx, or gastrointestinal mucosa.[39] Types I and II HAE result from a quantitative (type I) or qualitative (type II) deficiency in C1-esterase inhibitor (C1-INH), a protein controlling the activation of the complement pathway and the CAS: C1-INH acts as a natural inhibitor of FXIIa. In the absence of sufficient or functional C1-INH, FXIIa is excessively generated, leading to uncontrolled BK (vascular permeability mediator) overproduction and edema, as shown by murine models deficient in C1-INH.[39] In human patients, the understanding of this pathologic disease led to treatments directly targeting this condition, mainly C1-INH administration.[39]

HAE type III affects women almost exclusively: angioedema occurs despite C1-INH levels being normal and fully functional. It was shown to be an autosomal dominant disease associated with FXII gene point mutations.[39] The mechanisms for this disorder subtype are not well understood: FXII is supposedly abnormally activatable, although normal FXII levels are detected.

In all forms of HAE, overactivation of the CAS by FXII and overgeneration of BK is the central role of edema attacks.[39]

3.4.2. Sepsis

Sepsis is an exaggerated inflammatory response to a bacterial infection possibly leading to death when left untreated.[40] In the case of blood infection by bacteria, the CAS can be initiated through FXII activation by some bacteria components: these include lipopolysaccharides (for Gram-negative bacteria), peptidoglycans (for Gram-positive bacteria), teichoic acid, or PolyPs.[40,41] FXIIa then activates PK and FXI, leading respectively to BK production, and blood clot generation whose role is to trap involved pathogens. This immunothrombosis mechanism can lead to widespread microvascular thrombosis called disseminated intravascular coagulation (DIC), itself leading to widespread thrombosis and bleeding by consumptive coagulopathy, an excessive consumption of coagulation factors, platelets, and fibrinogen. Thrombosis occurring throughout the body leads to organ ischemia, hypoperfusion, and oxidative stress, failing the organs and contributing to the morbidity of sepsis, with death as a possible outcome.[40]

FXII could be an interesting inhibition target in the context of sepsis thrombosis. In a baboon model of *Escherichia coli* sepsis, Pixley[42] and Jansen[43] showed that FXII antibody inhibition attenuated terminal hypotension and reversible shock, whereas the control wild-type group developed irreversible lethal hypotension.

3.4.3. Alzheimer's disease

Alzheimer's disease is a progressive neurodegenerative disorder characterized by the accumulation of β-amyloid peptides in the brain.[44] The mechanisms by which they disrupt neuronal function *in vivo* are still unclear: neuroinflammation and neuronal dysfunction could result from changes in cerebral blood flow induced by a prothrombotic state, as supported by mouse models.[45] β-amyloid peptides have been shown to activate FXII *in vitro* and *in vivo* mouse models: FXII activation *via* the CAS triggers both the inflammatory pathway releasing BK, and the intrinsic coagulation pathway leading to the production of thrombin. These processes could promote neuroinflammation and said prothrombotic state.[45] Experimental data showed increased levels of FXIIa, fibrin and HK, and decreased levels of FXI, all signs of CAS activation and coagulation cascade initiation.[44,45]

3.5. Animal studies and human observations

Several studies have been conducted on genetically modified mice deficient in both alleles of the FXII gene ($FXII^{-/-}$).[27,46–48] FXII-deficient mice, like their human counterparts, develop normally, are healthy and fertile, and phenotypically indistinguishable from their wild-type littermates. They do not show spontaneous, abnormal, or excessive bleeding related to injury, and display a normal hemostasis process, despite a prolonged aPTT.[27,46–48] Moreover, *in vivo* $FXII^{-/-}$ mice

experiments revealed a crucial role for FXII in thrombosis: these mice are resistant to several models of induced thrombosis by a decrease in thrombus stabilization which prevents the occlusion of blood vessels. For instance, FXII-deficient mice exhibited moderate resistance for collagen and epinephrine-induced pulmonary thromboembolism,[27] $FeCl_3$-induced[27,47] and Rose Bengal-laser-induced[47] thrombosis by vessel injuries, and cerebral ischemic stroke.[48] These results suggest that FXII is dispensable for hemostasis, but is essential for pathological thrombus formation and stabilization *in vivo* that could induce thromboembolic complications, which could potentially be prevented by FXII inhibition.

Other studies on rabbits investigated FXII-related thrombosis in the presence of BCMD, namely catheters[49] and extracorporeal membrane oxygenation[50] (ECMO). Rabbit catheter-induced thrombosis triggered by the CAS was attenuated in plasma that is deficient in FXII and with selective FXIIa inhibition.[49] Similarly, activation of FXII with ECMO is significant: in the absence of anticoagulation medication, ECMO circuits become blocked within a few minutes, whereas inhibition of FXIIa with antibody 3F7 allowed the ECMO system to stay functional after 6 hours by limiting fibrin production and platelet deposition.[50] The same results have been achieved in baboon models.[51,52] Collagen-coated vascular grafts usually promote thrombus formation. However, FXII inhibition by monoclonal antibody 15H8 reduced fibrin formation and platelet accumulation to prevent blood clots.[51] Experiments on ECMO-induced thrombosis in baboons were completely similar to those in rabbits: the monoclonal antibody 5C12 inhibited FXIIa activity, which resulted in a significant decrease in thrombus formation.[52]

FXII deficiency in humans is not completely uncommon: heterozygosity for FXII deficiency was found in 2% of a series of 300 healthy blood donors.[53] The Asian population also seems to have lower FXII levels than occidental populations.[54] In general, FXII deficiency is inherited in an autosomal recessive pattern, where FXII levels in homozygous individuals are undetectable, and are between 20% and 60% of normal levels in heterozygous individuals.[55]

Similarly to mice, FXII deficiency does not induce spontaneous or excessive bleeding related to injury or surgical procedures in humans, although affected individuals display a prolonged aPTT. Some studies describe an association between FXII deficiency and spontaneous miscarriage, premature delivery, arterial and venous thromboses involving myocardial infarction and PE. However, these studies rely on small human samples, which results in the uncertainty of the definite cause and effect relationship.[55]

Considering these experimental results, FXIIa appears as a promising therapeutic target: its selective inhibition could present a safer alternative to current therapies by limiting bleeding risks.

3.6. Recent inhibitors

Multiple FXII(a) inhibitors have already been described in the literature and are currently in research. These include protein- and peptide-based inhibitors such as (monoclonal) antibodies and proteins derived from natural sources, but also RNA-based inhibitors (siRNA, antisense oligonucleotides) and more recently, small molecules.[30,34]

3.6.1. Protein-based inhibitors

3.6.1.1. Antibodies

Monoclonal antibodies such as 3F7[50], 15H8[51], and 5C12[52] have been briefly described in Section 3.5, where their thromboprotection in several models has been highlighted. 3F7 is a recombinant fully human antibody binding selectively into the FXIIa enzymatic pocket (IC_{50} = 13 nM). It is assumed to be a safe mode of anticoagulation, as it is expected to display minimal immunogenic potential in humans.[50] Affinity maturation of 3F7 was undertaken to enhance its potency in order to develop CSL312, a lead antibody now called Garadacimab: a 44-fold increase in affinity for FXIIa was measured with a picomolar affinity (K_D = 140 pM).[56] Garadacimab is currently undergoing a phase IV clinical trial for HAE (clinicaltrials.gov, ID: NCT06806657).[57]

Monoclonal antibodies 9A2 and 15H8 have been created to bind with the heavy chain of FXII to interfere with FXII activation: 9A2 is assumed to bind to the FnI and/or EGF2 domains, and 15H8 to the EGF2 and/or the kringle domains.[51] 15H8 showed a better inhibition towards FXII activity in baboon plasma and completely blocks the prothrombotic effect in FXII-deficient mice, whereas 9A2 only blocks it partially. Both 9A2 and 15H8 reduced fibrin formation in human blood perfused through collagen-coated tubes, although only 15H8 reduced fibrin formation in collagen-coated vascular grafts inserted into arteriovenous shunts in baboons, reduced fibrin and platelet accumulation downstream of the graft, and prolonged the aPTT of baboon and human plasmas.[51]

5C12 binds to the catalytic domain by recognizing both FXII and FXIIa of human and baboon enzymes, which potently inhibits FXIIa activity.[52] 5C12 also significantly reduced platelet deposition and fibrin formation in a baboon ECMO model, where the surfaces have been coated with collagen. Moreover, this monoclonal antibody inhibits contact activation-initiated clotting, which prolongs the aPTT and prevents thrombus formation.[52]

3.6.1.2. Proteins derived from natural sources

Corn trypsin inhibitor (CTI) which was first isolated from corn seeds and shown to inhibit trypsin, was later found to be a reversible FXIIa inhibitor (IC_{50} = 0.7 μM) used in blood samples to prevent initiation of the intrinsic pathway of coagulation in order to investigate TF-initiated coagulation (prothrombin time (PT) assay).[58] However, CTI does not appear selective *in vivo*, as inhibition of FXa, FXIa, thrombin, and plasmin has been observed.[30] CTI proved to attenuate catheter-induced thrombosis: *in vitro* experiments and *in vivo* rabbit models demonstrated longer clotting times for CTI-coated catheters since FXIIa activity was reduced, leading to a decrease in FXIIa-mediated blood coagulation. Catheter occlusion was also prolonged compared to unmodified catheters, proving that CTI-coated catheters are less thrombogenic than unmodified ones.[59]

Infestin-4 is a small protein initially isolated from insect *Triatoma infestans* with high inhibitory activity towards FXIIa (K_i = 128 pM).[60] However, Infestin-4 does not present a high elimination half-life nor a high selectivity for FXII, as inhibition for other blood serine proteases was described, namely plasmin, FVIIa, FIXa, FXa and thrombin (Ki in nM range).[30,60] To overcome these problems, a recombinant version has been developed: rHA-Infestin-4 fused with human albumin and Infestin-4 is a potent and selective FXIIa inhibitor *in vitro* and *in vivo*.[61] rHA-Infestin-4 appears to be a competitive FXIIa inhibitor that protects murine from thrombotic events by preventing platelet aggregation and thrombus formation after vascular injury, especially in a cerebral ischemia model.[61]

Ixodes ricinus contact phase inhibitor (Ir-CPI) is a Kunitz-type protein that was isolated from the salivary glands of the tick *Ixodes ricinus*.[62] By inhibiting the intrinsic coagulation pathway *via* the CAS and especially FXIIa, FXIa, as well as PK, Ir-CPI presents *in vivo* antithrombotic properties and prolongs the aPTT *in vitro*. Ir-CPI supposedly binds to an exosite of the activated forms of these enzymes, inducing steric hindrance that prevents protease activity. Venous thrombosis models were induced in FXII-deficient mice by collagen and epinephrine, and $FeCl_3$ injection: mice presented thromboprotection without any effect on hemostasis.[62]

3.6.1.3. Synthetic peptides

D-Pro-Phe-Arg-chloromethyl ketone (**PCK**) is a synthetic, chemically-modified tripeptide targeting FXIIa that has shown potential in murine models: FXIIa inhibition by PCK protected mice from induced cerebral edema and prevented development of cerebral infarction.[63]

FXII801 is a bicyclic peptide presenting strong inhibitory activity and selectiveness towards FXIIa, with an IC_{50} value of 1.6 nM.[64,65] Structures of described peptides are represented in Figure 12.

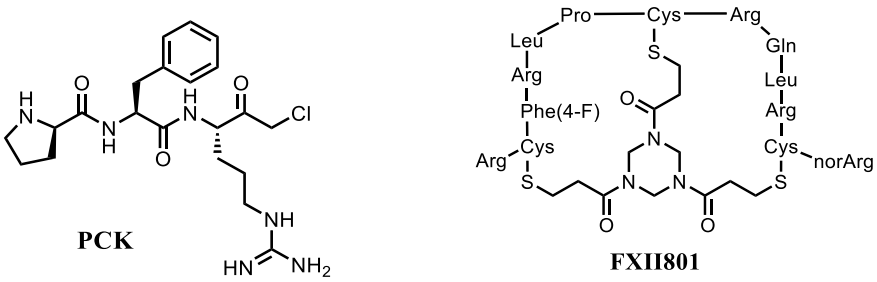

Figure 12. Structures of **PCK** and **FXII801**.

Protein-based inhibitors could represent an appealing strategy of inhibition, given their high bioavailability, effectiveness and selectivity for FXIIa, yet their production cost and the necessity of parenteral administration (usually by intravenous injection) could limit their clinical use, compared to small molecules delivered orally.

3.6.2. RNA-based inhibitors

3.6.2.1. Small interfering RNA

Gene silencing mechanisms such as RNA interference have lately emerged as a promising tool by using small interfering RNAs (siRNAs), small double stranded RNA analogs that target and degrade messenger RNA (mRNA) to prevent the associated protein expression.[66] Once delivered into the cell, siRNAs are bound by a multiprotein component called the RNA-induced silencing complex (RISC), which separates the two strands and allows the RISC to cleave the targeted mRNA.[67] ALN-F12 is a potent siRNA forming a duplex with GalNAc developed to target FXII mRNA in order to reduce plasma FXII levels.[68] *In vivo* murine experiments showed that administration of this conjugated entity resulted in dose-dependent suppression of FXII, prevented vascular permeability, and attenuated edema in HAE models.[68]

3.6.2.2. Antisense oligonucleotides

Antisense oligonucleotides (ASOs) are short DNA or RNA single-strands complementary to targeted mRNA. ASOs can bind with RNA in a target-specific manner to modify protein expression:[69] RNA cleavage by RNase H1 or RNA blockage by steric hindrance is induced to reduce protein production.[70] Mice and rabbit models confirm a decrease in FXII activity and can inhibit thrombus formation without affecting hemostasis, either induced by $FeCl_3$[71] or catheter-induced thrombosis.[49]

3.6.3. Small molecules

3.6.3.1. Aminotriazole scaffold

Over the years, Kalinin's research group has developed multiple potent FXIIa inhibitors based on the aminotriazole scaffold (Figure 13). One of their first and most potent compounds is **1** which presented a 29 nM inhibitory activity towards FXIIa.[64] They later developed compound **2**, which demonstrated selectivity for FXIIa and the lowest IC_{50} value of 7 nM.[72] In 2022, another compound, **3**, was developed based on the structure of the previous one (**2**): **3** presented an IC_{50} value of 28 nM against FXIIa, and in the micromolar range for thrombin, which presents a better selectivity for FXIIa compared to thrombin.[73] Binding studies by molecular modeling and mass spectrometry allowed the authors to hypothesize on the mechanism of inhibition of these aminotriazole compounds: they are presumed covalent inhibitors, since a change of mass of FXIIa has been measured after putting the enzyme and the inhibitor together. Ser195 seems to act as a nucleophile attacking the carbonyl moiety to form a tetrahedral intermediate stabilized by the oxyanion hole (backbone hydrogens of Gly193 and Ser195). Furthermore, this acyl moiety appears to be hindered enough and exhibits adequate geometry to present a binding preference towards FXIIa.[64,73]

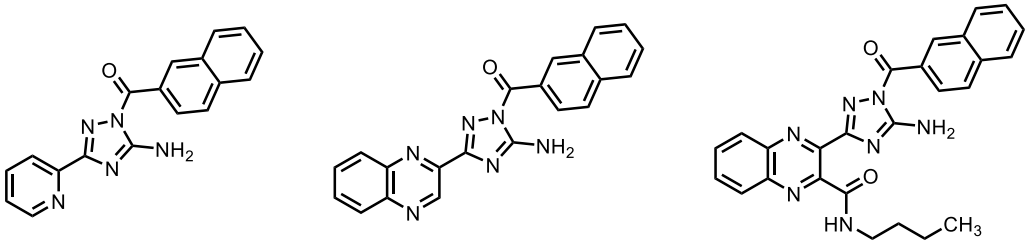

1: IC_{50} = 29 nM **2**: IC_{50} = 7 nM **3**: IC_{50} = 28 nM

Figure 13. Compounds developed in Kalinin's research group.[64,72,73]

3.6.3.2. Coumarin scaffold

Figure 14 presents several molecules based on a coumarin scaffold which have been researched in our institution. Among them lies compound **4** developed in L. Pochet's research group, which presented a 5 µM IC_{50} inhibition towards FXIIa.[74] Similarly, molecule **5** (RF1) contains a coumarin scaffold and a phenyl guanidine entity: it is selective for FXIIa with an IC_{50} value of 6 µM.[75] Although these molecules are selective for FXIIa, their micromolar inhibition shows that these compounds require more modulations. Another series of compounds based on coumarins has been developed to increase the potency and selectivity towards FXIIa: **6** and **7** exhibit an IC_{50} value of 62 nM and 98 nM, respectively.[75]

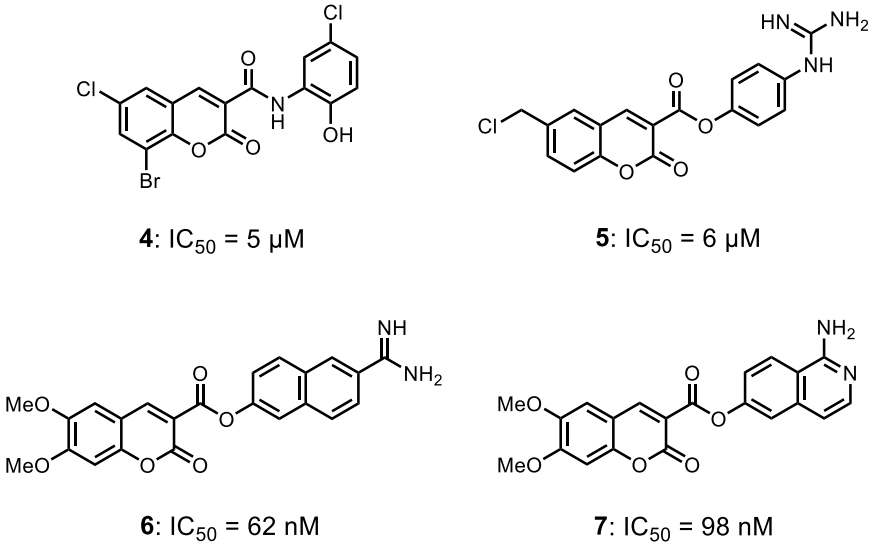

Figure 14. Compounds developed in L. Pochet's research group.[74,75]

These molecules contain another type of scaffold, 6-hydroxy-2-naphthimidamide for compound **6** and 1-aminoisoquinoline for compound **7**. These types of fragments (Figure 15), 6-hydroxy-2-naphthimidamide (**8**) and 1-aminoisoquinoline (**9**) present selectivity for FXIIa and a comparable inhibitory activity with one order magnitude higher than benzamidine (**10**).[75] While their inhibition values do not seem satisfactory as they are, these fragments constitute a promising scaffold for the development of potent and selective FXIIa inhibitors with encouraging IC_{50} values, where fragment **9** presents a better selectivity for FXIIa.[75]

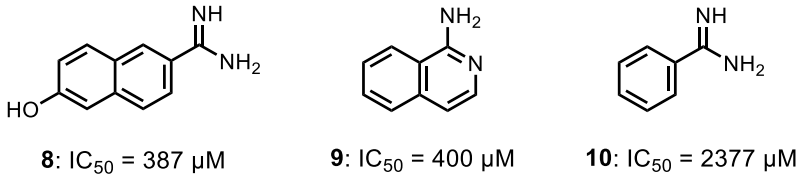

Figure 15. 6-hydroxy-2-naphthimidamide (**8**), 1-aminoisoquinoline (**9**) and benzamidine (**10**) fragments.

OBJECTIVES AND STRATEGIES

All this research points out that FXIIa appears as a promising therapeutic target to prevent thrombosis while minimizing interference with hemostasis, especially in the context of BCMD, but also other diseases such as HAE, sepsis and Alzheimer's. Commonly given anticoagulants unfortunately lead to an increased hemorrhagic risk as well as other possible undesired side effects. Several FXIIa inhibitors such as peptides, antibodies, and siRNAs have been described and appear very effective, but they present a significant cost, complexity of synthesis, and limitations in terms of parenteral administration. The synthesis of low-molecular-weight FXIIa inhibitors that are potent, selective, and compatible with oral administration needs to be explored. To the best of our knowledge, the development of simple, inexpensive and orally administered organic compounds as FXIIa inhibitors has been scarcely described with a lack of clinical tests, despite being of great interest. Due to its nature as a serine protease, the inhibition of FXIIa could be done selectively by targeting, through adequate interactions, the oxyanion hole and its pockets containing interesting residues.

The goal of this work is to attempt the synthesis of benzamidine-based small-molecular-weight inhibitors that target FXIIa selectively and efficiently with a nanomolar inhibitory activity, especially through interaction with its S3 pocket. Figure 16 presents the structure of potential lead compounds targeting different pockets, where molecule **11** will ultimately be synthesized with diverse S3 groups.

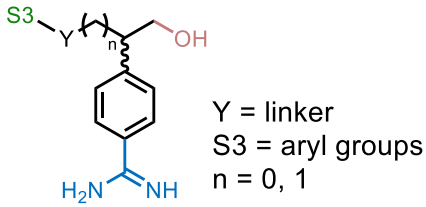

11

Figure 16. Structure of possible lead compounds targeting the oxyanion hole, the S1 and S3 pockets.

The base of molecule **11** is benzamidine, which is a known S1-binding fragment, as it has previously been crystallized with FXIIf (Figure 10). Benzamidine was proven to have good affinity for Asp189 of the S1 pocket: it represents an adequate base to extend fragments to other pockets. A first extension towards the oxyanion hole will be achieved *via* an alcohol moiety in order to mimic the enzyme's tetrahedral intermediate. The rest of the molecule will then be extended using a linker to reach into the S3 pocket of FXIIa: this linker will be, as a first approach, an amide entity. Residues Tyr99 and Trp215 of the S3 pocket will also be targeted

through the grafting of aryl fragments (S3 groups) with different electronic effects, and changed according to the obtained inhibition values. The absolute configuration of the benzylic carbon will also be investigated: docking studies[76] pointed out a stereochemical preference for the S absolute configuration of this benzylic carbon (molecule **12** of Figure 17), which is supposed to be adequate to be selective for FXIIa. The anti relative configuration between the S and R enantiomer has also been evaluated in these docking studies. Both enantiomers would still be independently synthesized and evaluated.

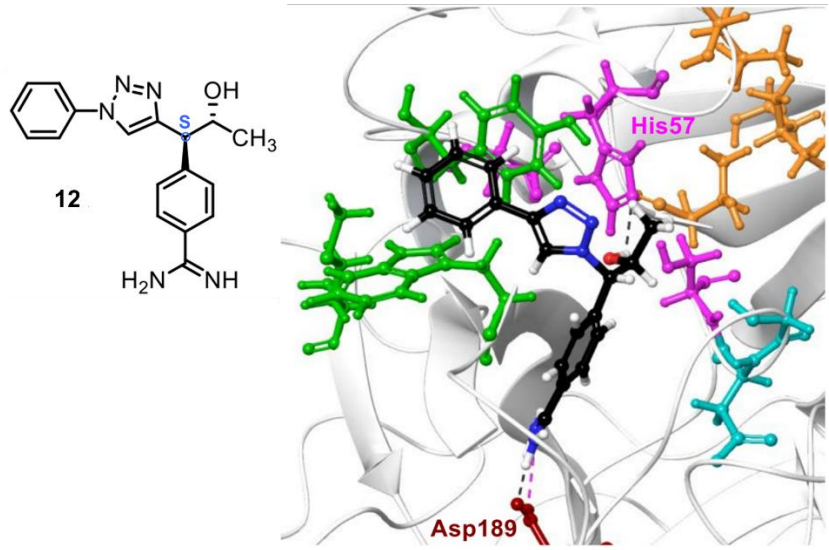

Figure 17. Structure of FXIIa inhibitor **12** and docking of compound **12** within the binding site.[76]

Enzymatic assays will be conducted by an IC_{50} assay to evaluate the inhibitory activity of both enantiomers of compounds **11**, as represented on Figure 18. The most potent compounds will be identified.

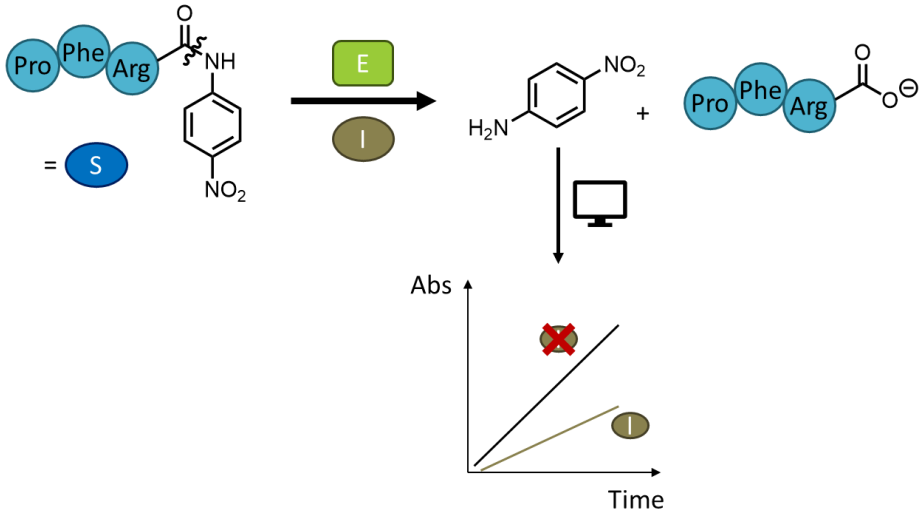

Figure 18. Schematic representation of the chromogenic IC_{50} assay used to evaluate the inhibitory activity of obtained compounds **11**. The enzyme's substrate is a peptide analogue that, when cleaved, presents an activity in UV-Vis, which can be measured at different concentrations to evaluate IC_{50} values.

Furthermore, the anticoagulant profile of obtained compounds will be determined: these molecules will undergo the aPTT assay to evaluate clotting times *via* the intrinsic pathway of coagulation, as well as the PT assay to determine if they exhibit interference with the extrinsic pathway. Both assays evaluate clotting times *in vitro* of platelet poor plasma: the aPTT requires a FXII activator such as silica, kaolin or ellagic acid, to which phospholipids and calcium will be added. Similarly, the PT assay requires TF, phospholipids and calcium. Scheme 1 presents a first synthetic route imagined to obtain those potential lead compounds.

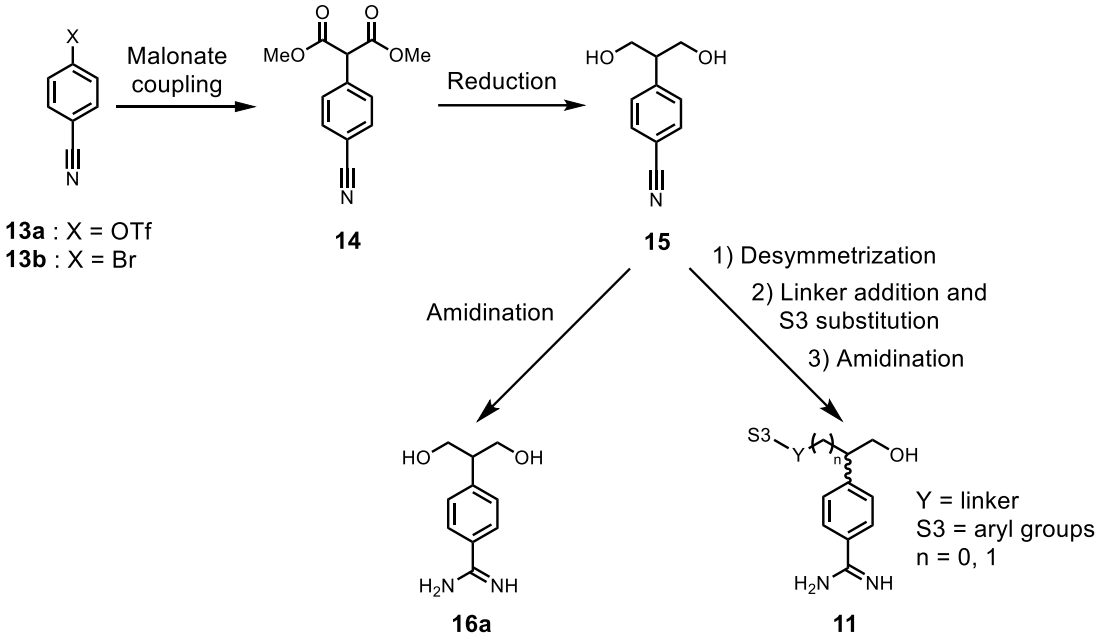

Scheme 1. Synthetic route to obtain possible lead compounds targeting the oxyanion hole, the S1 and S3 pockets.

The synthesis will start with a coupling partner (**13**) to achieve a metal-catalyzed cross-coupling reaction with dimethyl malonate. Intermediate **14** will then be reduced to a diol. These two first steps appear easy to set up and convenient: malonate couplings have been described in the literature, and the reduction step of a diester seems straightforward. Compound **15** will then undergo an amidination step to obtain molecule **16a** as a mimetic of the tetrahedral intermediate, a first compound that will be tested through enzymatic assays to evaluate its inhibitory activity: molecule **16a** should target the oxyanion hole and the S1 pocket, and should therefore have a lower IC_{50} than benzamidine (**10**). The rest of the synthesis will be performed from molecule **15** that will be desymmetrized, extended with a linker, and finally amidinated. The nitrile group will be preserved for the whole synthesis and will only be transformed into an amidine group at the end for the enzymatic tests in order to avoid any purification complication.

Although the objective of this work is to target the oxyanion hole, the S1 and S3 pockets, another approach could be developed to target pocket S1* by a sulfate analogue, and pocket H1 by aliphatic chains, starting from the common intermediate **15**. Other researchers in our group are working on these strategies.

RESULTS AND DISCUSSION

1. SYNTHESIS OF A COUPLING PARTNER

Before diving into the malonate cross-coupling reaction, a first coupling partner had to be obtained, **13a** of Scheme 2, by a triflation reaction of a phenol.

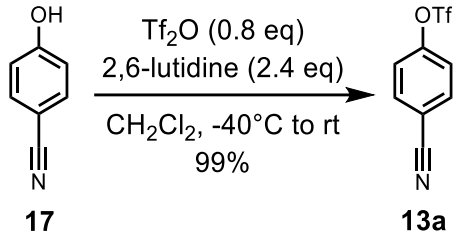

Scheme 2. Triflation reaction of 4-hydroxybenzonitrile **17**.

The triflation step based on the protocol of Uchiyama *et al.*[77] from molecule **17** to **13a** was successfully achieved with a 99% yield. The phenol acts as the nucleophile to attack trifluoromethanesulfonic anhydride, a strong electrophile. 2,6-lutidine deprotonates the protonated phenol: its steric hindrance and non-nucleophile character render it an adequate base. TLC monitoring showed that some phenol **17** remained, as only 0.8 equivalents of trifluoromethanesulfonic anhydride were added. The NMR data confirms the formation of the desired product **13a**: the ^{1}H NMR shows a shift of the two aromatic peaks and the disappearance of the phenol hydrogen, and the ^{19}F NMR only shows a single peak at -72.5 ppm. Once this starting material **13a** was obtained, tests for the coupling protocol could be carried out.

2. MALONATE CROSS-COUPLING REACTION

Scheme 3 presents a first cross-coupling protocol to substitute dimethyl malonate on the aryl compound **13a**, following the patent of Karnik *et al.*[78] to try to obtain molecule **14**. This protocol uses NaH as the base, copper(I) as the catalyst, and NMP as the ligand and the solvent. However, no product **14** was identified by ^{1}H or ^{13}C NMR: the starting material **13a** and the phenol **17** were retrieved. No further investigations were conducted to determine the reason for this failed reaction: this protocol was thus abandoned.

Another metal source was used, following the works of Hartwig and Buchwald of Pd-catalyzed cross-coupling reactions. Their work mainly examines the arylation of amines but is also suitable for the arylation of malonates, which has already been described.[79,80] Both starting materials **13a** and **13b** (Table 1) have been used for these reactions to determine the best conditions. Table 1 summarizes the different reaction conditions for the Pd-catalyzed cross-

coupling of **13** to **14**, following the publication of Semmes *et al.*[80] and the patent of Pintchovski and Shrader[81] with some adjustments.

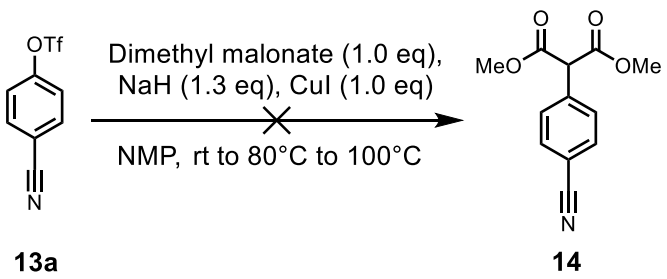

Scheme 3. Copper-catalyzed malonate cross-coupling reaction of **13a**.

Table 1. Different reaction conditions for the Pd-catalyzed cross-coupling of **13** to **14**.[a]

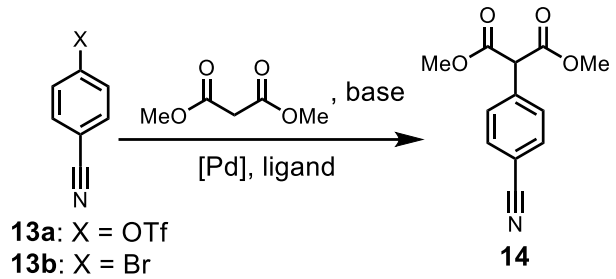

Entry	Starting material	Base	Pd source	Ligand	Time (h)	Yield (%)
1[b]	**13a**	NaH	$Pd(dba)_2$	$P(tBu)_3HBF_4$	68	/
2		K_3PO_4	$Pd(OAc)_2$	JohnPhos	3	39
3				SPhos	24	9
4[c]				XPhos	2	82
5				*t*BuXPhos	25	/
6[d]	**13b**	NaH	$Pd(dba)_2$	$P(tBu)_3HBF_4$	45	/
7[b]					67	/
8		K_3PO_4	$Pd(OAc)_2$	JohnPhos	26	10
9[c]				XPhos	4	82

[a] Reactions conditions (unless mentioned otherwise): in dry toluene using **13** (1.0 eq), dimethyl malonate (1.1 eq), K_3PO_4 (3.0 eq) or NaH (1.2 eq), [Pd] (0.10 eq), ligand (0.20 eq) at 125°C. [b] Dimethyl malonate (1.2 eq) at 70°C. [c] $Pd(OAc)_2$ (0.05 eq), XPhos (0.10 eq). [d] Dimethyl malonate (1.2 eq), $Pd(dba)_2$ (0.01 eq), $P(tBu)_3HBF_4$ (0.02 eq) at 70°C.

Reactions where $P(tBu)_3$ was used as the ligand (entries 1, 6 and 7) did not afford the desired product at all. With NaH as the base, bubbles were observed and could confirm that the dimethyl malonate was indeed deprotonated. However, even after almost three days of reaction, the TLC monitoring as well as the NMR of the crudes showed that no product **14** was obtained. The unsuccessful reactions could be explained by the low solubility of $P(tBu)_3HBF_4$ in toluene, but no further investigation was carried out to determine the reason for these failed experiments.

Since this protocol did not yield acceptable results, Buchwald's dialkylbiaryl phosphine ligands were tested. Entries 2 and 8 using JohnPhos as a ligand showed that the desired product was obtained in low yield (39% and 10%, respectively), which is an improvement compared to Hartwig's phosphine ligand. A control reaction (Scheme 4) was set up with 1-bromo-4-methylbenzene (**18**) to check whether the nitrile group interfered in the coupling reaction, or if the JohnPhos ligand was unsuitable. The obtained yield of 13% does not represent a significant improvement compared to benzonitrile moiety **13b**: the nitrile group does not seem to interfere much in the reaction. Moreover, brominated starting materials could be less compatible with JohnPhos than triflated ones, compared to the difference of yields between **13a** (39%) and **13b** (10%). In any case, better reaction conditions need to be researched to increase to an acceptable yield, as the ligand plays an important role in these cross-coupling reactions.

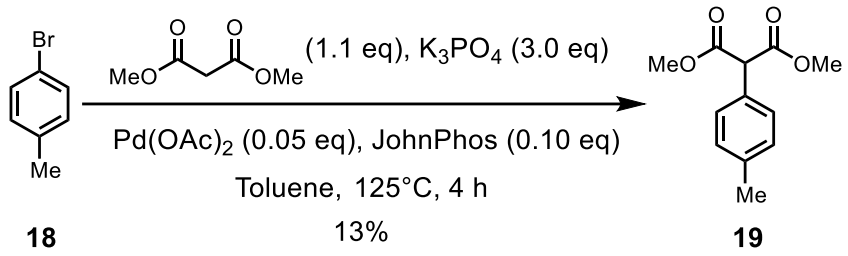

18 **19**

Scheme 4. Palladium-catalyzed malonate cross-coupling reaction of 1-bromo-4-methylbenzene **18**.

A screening of a few ligands (SPhos, XPhos and *t*BuXPhos, c.f. Additional structures) has been carried out with **13a** to obtain more acceptable yields with the same protocol as JohnPhos (entries 3-5 of Table 1). XPhos (entry 4) appears to be the most appropriate ligand for this coupling reaction by exhibiting an excellent yield of 82%. Reactions with SPhos and *t*BuXPhos respectively either gave poor yield (9%) or no product **14** was observed (entries 3 and 5, respectively). Entry 9 points out that the XPhos procedure also works on starting material **13b** with an identical yield of 82%: the nature of the starting material does not matter. An innovative, easy to set up and effective protocol inspired from the Pintchovski and Shrader[81] procedure has therefore been identified with K_3PO_4, $Pd(OAc)_2$ and XPhos, and works regardless of the leaving group of the coupling partner within only a few hours' time. The structure of **14** was confirmed by XRD analysis (c.f. Additional structures). For this specific cross-coupling reaction, Buchwald-type ligands allowed to obtain the desired product, unlike Hartwig's ligands. However, this approach performs more efficiently on a small scale: upon scale-up, a decrease in yield is observed, with values dropping to over 60%, or even as low as 50%. Further investigation is required to better understand these limitations, potentially by adjusting the catalyst loading, dilution, or modifying other conditions.

3. SYNTHESIS OF THE COMMON INTERMEDIATE

Once the aryl malonate **14** was obtained, several protocols were followed to reduce it to the diol **15** (Table 2). Choosing an adequate reducing agent is crucial to only reduce the esters without interfering with the nitrile. In the literature, $LiBH_4$ has been proved to fulfill this role,[82,83] but other reducing agents have been tested as well. Table 2 summarizes the different reactions conducted and their conditions, with adequate references to the protocols applied with some adjustments.

Table 2. Different reaction conditions for the reduction of the aryl malonate **14** to **15** and **20**.

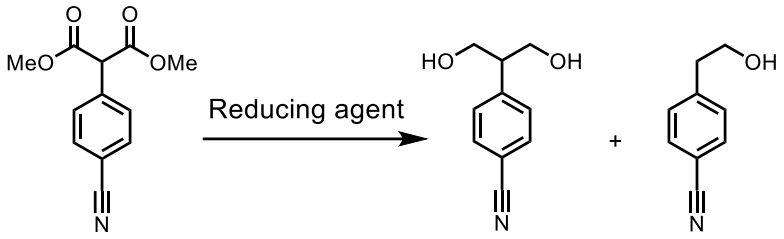

14 **15** **20**

Entry	Reducing agent (eq)	Additive (eq)	Solvent	Temp. (°C)	Time (h)	Yield of **15** (%)	Yield of **20** (%)	Refs
1	$LiBH_4$ (2.0)	MeOH (4.0)	THF_{dry}	rt	22	/	/	[84]
2	$LiBH_4$ (3.6)	/	THF_{dry}	40 → 60	6	/	/	[85]
3	$LiBH_4$ (3.0)	/	THF_{dry}	0	16.5	/	/	[86]
4	$LiBH_4$ (6.0)	MeOH (6.0)	Et_2O_{dry}	0 → rt	4	/	13	[87]
5	$LiAlH_4$ (4.0)	/	THF_{dry}	0 → rt	2.5	/	/	[88]
6	DIBAL-H (4.0)	/	$Toluene_{dry}$	-78 → -45	3	/	/	[89]
7	$NaBH_4$ (6.0)	/	MeOH	rt	23	29	50	[90]
8	$NaBH_4$ (8.0)	/	H_2O:dioxane (1:1)	rt	16	15	45	[91]

Entries 1-6 did not yield the desired diol **15**. Entries 1-4 show that adding more equivalents of $LiBH_4$, methanol or heating the reaction mixture did not change the outcome. The starting material and unidentifiable products were retrieved for entries 1-4, where **14** was present in majority for entries 1-3, meaning that the starting material was scarcely converted. It is supposed that a mono-reduction product may have been formed for the reaction of entry 1, but no further investigations confirmed this hypothesis. Although the crude of entry 4 seemed to contain multiple products, a low yield of alcohol **20** was able to be obtained after purification: the use of this product will be further explained below.

A test reaction (Scheme 5) was conducted to determine if the $LiBH_4$ powder has possibly deteriorated over time.

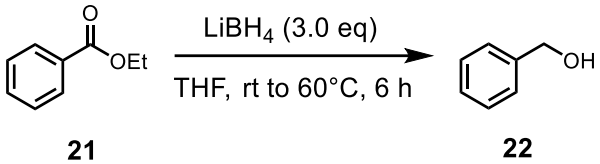

Scheme 5. Reduction of ethyl benzoate (**21**) into benzyl alcohol (**22**) with $LiBH_4$.

After six hours of reaction heated to 60°C and 3.0 equivalents of $LiBH_4$ added, alcohol **29** started appearing in TLC monitoring: the reaction was stopped right after, the product was not purified, thus no yield was obtained. These conditions are harsh and should not be necessary for ester reduction with $LiBH_4$: reactions are typically conducted at 0°C or room temperature, with 2 equivalents of $LiBH_4$ per ester. Besides, reactivity of the $LiBH_4$ powder was tested in water: contrary to its sodium analogue $NaBH_4$, $LiBH_4$ powder appeared unreactive and did not produce any bubbles when added to water. This could confirm that the $LiBH_4$ used was indeed deteriorated. Other researchers in our group performed similar coupling reactions with a new batch of $LiBH_4$, but the same unsuccessful results were obtained. This new $LiBH_4$ also appeared unreactive to water and paper towels.

Considering the unsatisfactory results yielded by $LiBH_4$, other conditions were therefore tested (entries 5-6 of Table 2). Unfortunately, these conditions also did not allow us to obtain the desired diol **15**. Possible products of the crudes of these reactions were much more unidentifiable than for entries 1-4. Nevertheless, in both cases, the malonate reduction was not complete: aldehydes peaks were identified around 10 ppm in ^{1}H NMR and 190 ppm in ^{13}C NMR, and ester peaks were still present around 165 ppm of ^{13}C NMR (Figure 19). In addition to that, the nitrile group of the starting material was reduced to the corresponding amine in the case of $LiAlH_4$ (entry 5), as shown by the disappearance of the ^{13}C peak around 118 ppm (Figure 19b).

A hypothesis for these unwanted side reactions could be the following: $LiAlH_4$ and DIBAL-H do completely reduce nitriles to amines that can complex with the aluminum species, lowering the reactivity of the reducing agent. Thus, the intermediate formed is not reactive enough to completely reduce the esters to alcohols, which could explain the multiple peaks in the carbonyl region. Strong reducing agents appear unsuitable for this sensitive step.

In entries 7-8 of Table 2, $NaBH_4$ was used as a last resort. Against common knowledge stating that $NaBH_4$ is not a reducing agent strong or fast enough to reduce esters, it appears to unexpectedly yield the most promising results in our case, allowing us to obtain the desired diol **15** in modest yields. Alcohol **20** was also formed in moderate yields as a side product: the ratio steers towards this alcohol for every reaction with $NaBH_4$. This product most likely comes from a decarboxylation reaction of the starting material **14** due to the acidity of the α-hydrogen,

followed by the reduction step. Although molecule **20** was not expected at first, it could prove to be interesting for enzymatic tests. Due to the higher yields of both products, the protocol of entry 7 was selected for the rest of the synthesis. By this reduction protocol, two interesting products, **15** and **20**, are obtained in a single step in moderate yields.

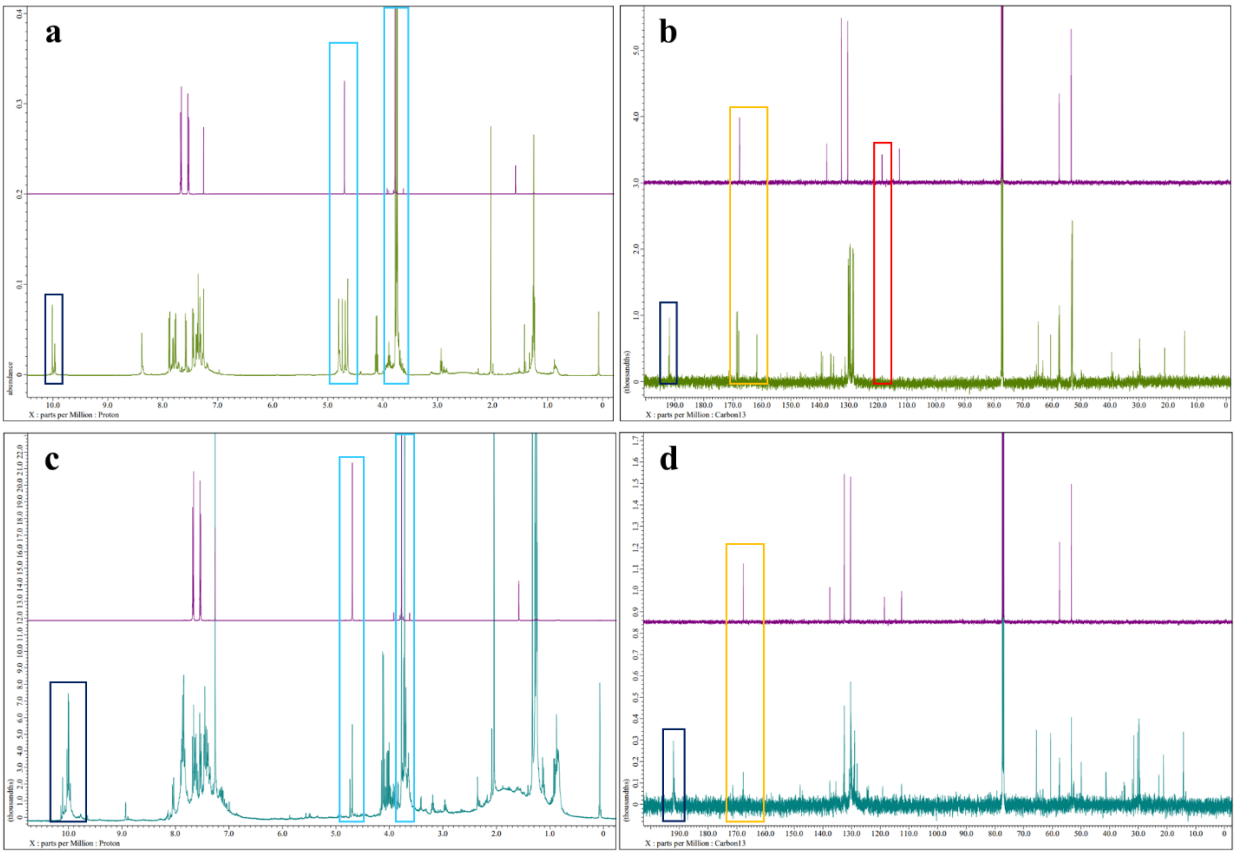

Figure 19. ^{1}H (**a** and **c**) and ^{13}C (**b** and **d**) NMR spectra of starting material **14** (in magenta), crude of entry 5 (**a**-**b**, in green) and crude of entry 6 (**c**-**d**, in cyan).

4. CONVERSION OF NITRILE TO AMIDINE

Two interesting products have been obtained in hope of targeting the oxyanion hole: these products could easily undergo the conversion of a nitrile to an amidine. With the aim of evaluating the inhibitory activity of a first molecule to compare it to benzamidine (**10**) to determine whether it presents a better IC_{50} value and if the alcohol entity adds value to the effectiveness of these potential inhibitors, molecule **20** was protected or used as it is to undergo an amidination step (Scheme 6). By targeting the oxyanion hole, IC_{50} values should be lower than benzamidine, due to a better binding affinity with FXIIa.

Three reactions were conducted: one with **20** was left at room temperature overnight, and the other two with **20** or **23** were heated at 60°C for a few hours. The starting material was retrieved after the first reaction overnight: this confirms that heating is necessary in order to achieve

conversion. Indeed, upon heating, TLC monitoring showed complete conversion of the starting material after a few hours. However, the amidine was not retrieved either with the unprotected or protected alcohol, most likely due to loss of product during the work-up process: very little mass was obtained in both cases. This protocol was adapted from literature[92] by a previous researcher in our group.[76] It is possible that the obtained compound was either degraded of lost during the filtration step. Unfortunately, due to lack of starting material, this reaction could not be continued further.

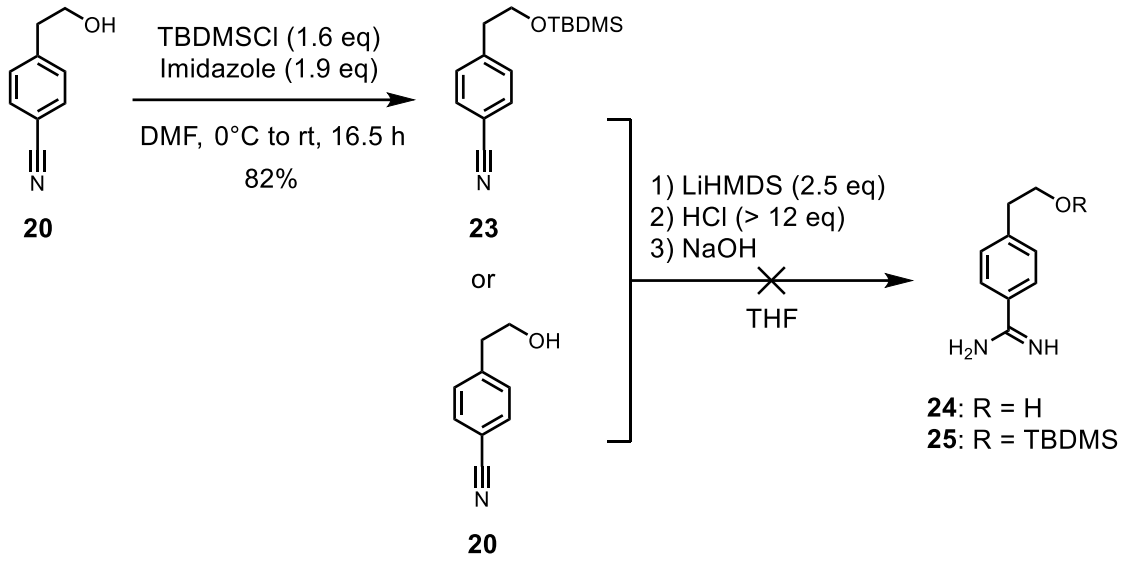

Scheme 6. Amidination reactions carried out for substrates **20** and **23**.

Although this amidination step was not successful for the conversion of alcohol **20**, this protocol was also applied, with some adjustments, to diol **15** (Scheme 7), and complete conversion was also observed. The reaction work-up was carried out differently, which seemed to allow us to obtain the desired amidine **16b** as a salt. The mass of **16b** was confirmed by HRMS (m/z calculated for $[M]^+$ 195.1128, found 195.1124), yet no nitrile (118 ppm) or amidine (around 160 ppm) peak seems to appear on the ^{13}C NMR spectrum (Figure 20).

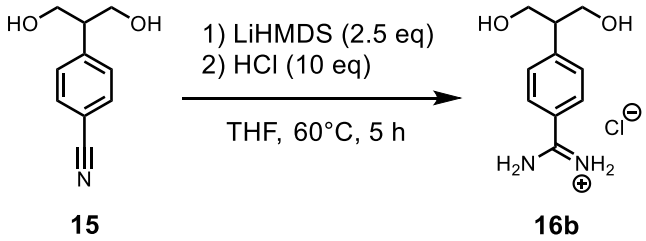

Scheme 7. Amidination reaction carried out for substrate **15**.

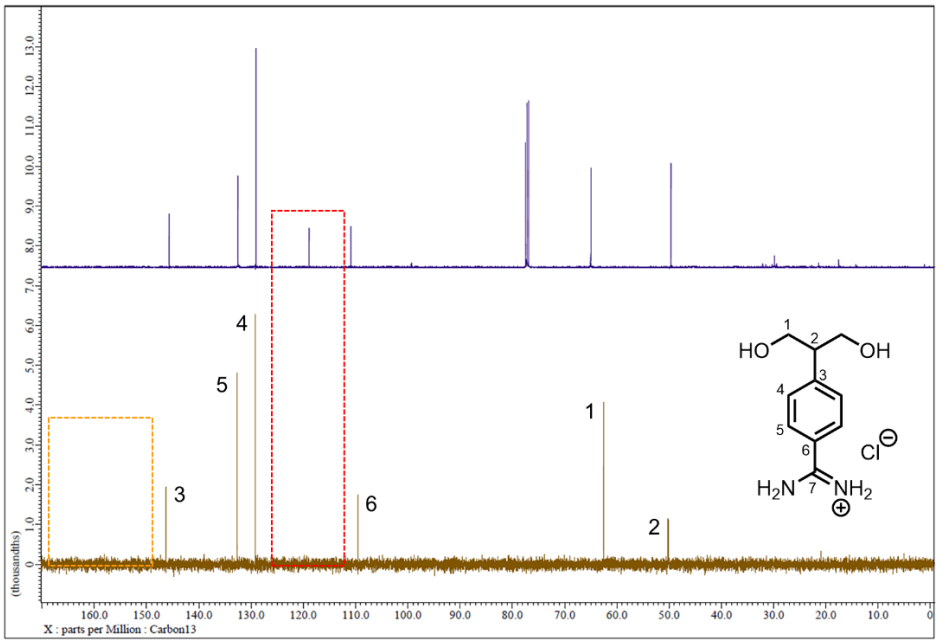

Figure 20. ^{13}C NMR spectra of starting material **15** (in deep blue) performed in $CDCl_3$ and compound **16b** (in brown) performed in D_2O. The nitrile peak of **15** (red dotted rectangle) seems to disappear at 118 ppm when converted into **16b**, and no typical amidine peak seems to appear around 160 ppm (orange dotted rectangle).

5. CHANGE OF STRATEGY

Although the reduction step allowed to obtain two interesting products **15** and **20**, other synthetic strategies starting from molecule **14** have been envisioned to enhance their yield (in Scheme 8).

Another strategy could consist in forming a silyl enol ether that will undergo an aldol reaction to ultimately be reduced to the desired diol **15**. It is not represented on Scheme 8, but this strategy could be applied to aldehyde **29** instead of silyl enol ether **27**. The aldol reaction step from **29** to **30** would be proline-catalyzed to obtain the two desired enantiomers. The aldehyde moiety would then be protected to substitute the alcohol by an amine through a Mitsunobu-type reaction, to form molecule **31**. After a reduction step to form compound **32**, the rest of the synthesis could take place as in Scheme 1, by a linker addition and the final amidination step.

The first step of Scheme 8 was followed to obtain the decarboxylated ester **26**, as represented in Scheme 9, following the protocol of Ates *et al.*[93] with some adjustments.

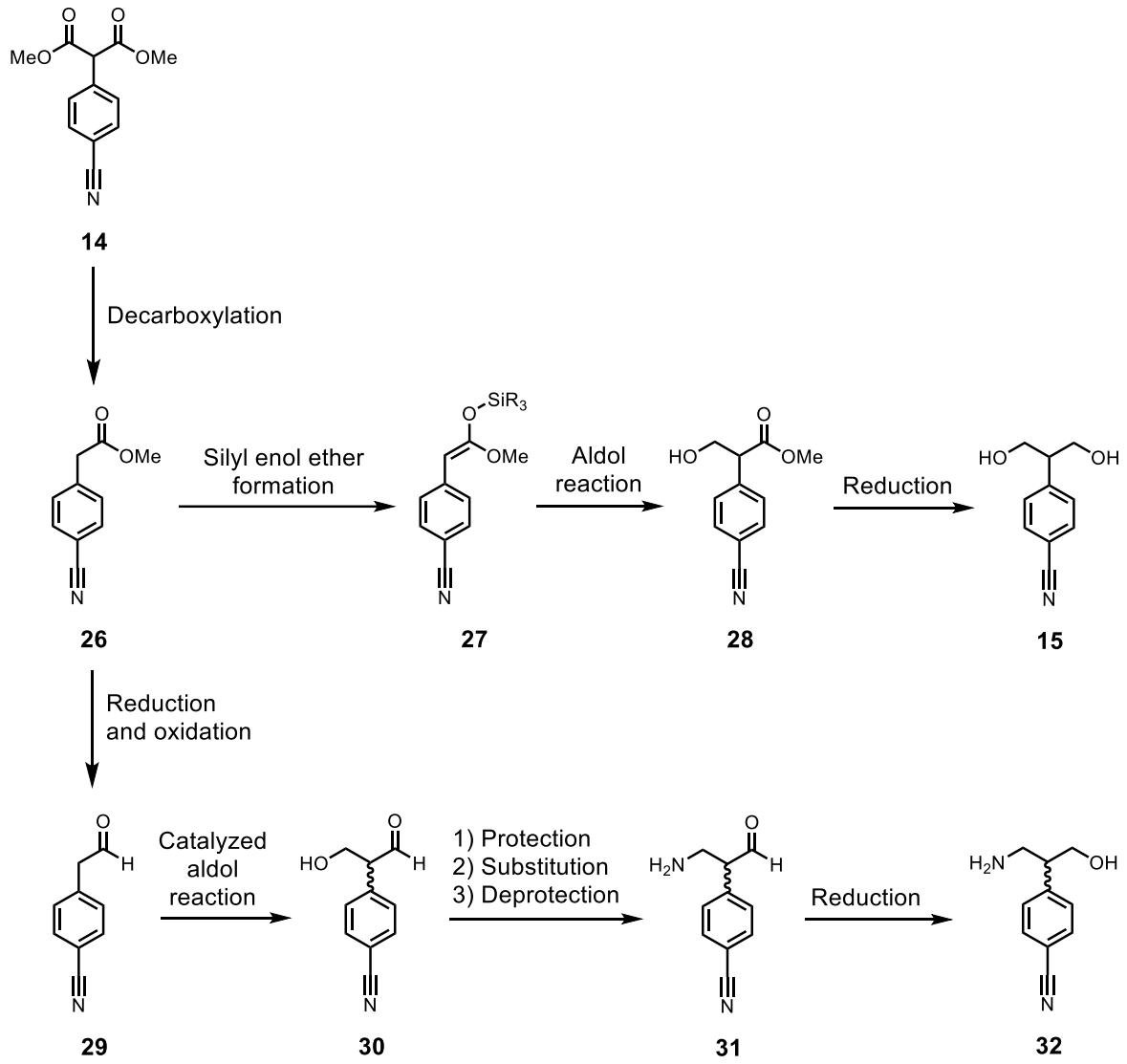

Scheme 8. Other possibles synthetic routes to obtain lead compounds.

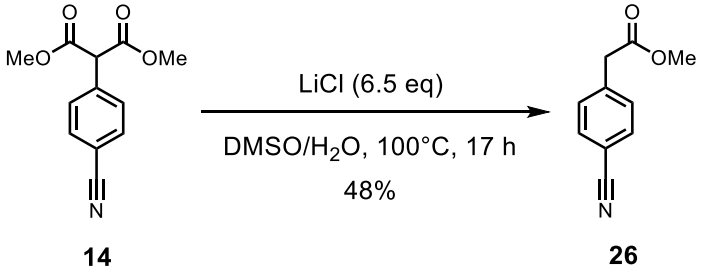

Scheme 9. Decarboxylation step from molecule **14** to **26**.

Conversion was not complete and the obtained yield was moderate, which could be explained by a lower reactivity of LiCl used, caused by hydration over time. The desired product **26** was nonetheless obtained and purified.

From this point, the synthetic sequence was envisaged to be continued by the reduction of **26** to obtain **20**, which will be oxidized to access the aldehyde intermediate **29** of Scheme 8, before proceeding with the rest of the synthesis.

CONCLUSIONS AND OUTLOOKS

1. GENERAL CONCLUSIONS

Over the past decades, FXIIa has emerged as a particularly promising therapeutic target for the prevention of thrombosis, as its inhibition appears to prevent thrombus formation while maintaining physiological hemostasis. Unlike conventionally given anticoagulants, which are associated with significant bleeding risks and other possible side effects, FXIIa inhibition holds promise for safer antithrombotic therapies: this is especially the case for BCMD-induced thrombosis, but also in other pathologies involving the CAS such as HAE, sepsis, and Alzheimer's disease. While several biological FXIIa inhibitors have demonstrated high efficiency, such as antibodies, proteins, synthetic peptides, and RNA-based strategies, their clinical application remains limited by high costs, synthetic complexity and especially parenteral administration. In this context, the development of low-molecular-weight FXIIa inhibitors that are potent, selective and potentially orally deliverable appears as an attractive alternative.

The objective of this work was to contribute to this approach by the synthesis of benzamidine-based small molecule FXIIa inhibitors designed to interact with the S1 pocket, the oxyanion hole, and the S3 pocket of the enzyme, as shown on Figure 16. Benzamidine was selected as a well-established S1-binding fragment, providing foundation for fragment extension towards other pockets. The hydroxy group will be in charge of mimicking the tetrahedral intermediate of the enzyme's transition state. A linker will enable the grafting of aromatic groups interacting with residues Tyr99 and Trp215 of the S3 pocket. This strategy was supported by previous docking studies, where a stereochemical preference for the S enantiomer of the benzylic carbon was observed, and was planned to be evaluated experimentally.

From a synthetic point of view, this work led to the successful development of an innovative and efficient Pd-catalyzed malonate cross-coupling reaction between aryl triflates or bromides with nitrile as a non-participating functional group. Through screening of different ligands, XPhos emerged as a particularly effective ligand in selected conditions with $Pd(OAc)_2$ and K_3PO_4, to proceed in high yields and short reaction times. The desired malonate compound was easily accessed for further synthesis.

The subsequent reduction of the obtained malonate to the corresponding diol proved to be a challenge. Several classical reducing agents reported in the literature for ester reduction were investigated, such as $LiBH_4$, $LiAlH_4$ and DIBAL-H, but none allowed clean conversion to the desired diol **15** while preserving the nitrile group untouched. Side reactions, incomplete

conversions and undesired nitrile reduction were consistently observed, highlighting the sensitivity of this reaction. Interestingly, $NaBH_4$, despite being generally considered too mild for ester reduction, afforded the desired diol **15** in modest yields, alongside a decarboxylated alcohol formed as a side product. Although not initially anticipated, this outcome provided access to two potentially relevant intermediates in a single step.

Attempts to convert the nitrile groups of these alcohol intermediates into the corresponding amidines were not particularly successful, although this step is necessary to evaluate their inhibition. While complete conversion of nitriles was observed by TLC monitoring upon heating, isolation of the amidine products proved challenging, likely due to losses during work-up. Nevertheless, an amidine derived from the diol **15** was obtained after a different work-up method was executed.

2. PERSPECTIVES

While a complete lead compound could not be synthesized within the time frame of this work, this project highlights the potential and the challenges associated with the chosen approach to obtain low-molecular-weight FXIIa benzamidine-based inhibitors. However, synthetic insights and alternative pathways were identified, providing a strong basis for future optimization.

As a first straightforward continuation, the amidination step could be optimized for molecule **20**, following the protocol used for amidine **16b** in order to obtain, alongside molecule **16b**, two compounds that could be evaluated in biological inhibition assays. Alcohol **20** could be accessed in a more controlled manner, possibly by an optimized decarboxylation step as envisioned in Scheme 9, followed by a reduction reaction.

In parallel, further efforts should focus on obtaining the desired diol **15**. As suggested on Scheme 8, one possible strategy would involve an initial optimized decarboxylation step, followed by the formation of a silyl enol ether which allows a subsequent aldol reaction, and a final reduction step to access diol **15**. Enzymatic desymmetrization using lipases such as PPL, CAL-B, PSL, etc. could then be performed to obtain both enantiomers, which would allow the investigation of the stereochemical considerations on FXIIa inhibition. Once the diol is obtained, the rest of the synthesis could proceed as described in Scheme 1, possibly by a Mitsunobu reaction followed by a Staudinger reaction to obtain the corresponding amine.

Alternatively, another pathway could be considered by performing a proline-catalyzed aldol reaction of aldehyde intermediate **29**, where the resulting alcohol would be substituted to an amine by a Mitsunobu-Staudinger reaction, and the aldehyde ultimately reduced to access an

amine compound useful for linker insertion. This strategy would avoid enzymatic desymmetrization and introduce chirality by a proline-catalyzed asymmetric step.

In both cases, the resulting intermediate (compound **32**) could react with a series of acyl chlorides bearing different aromatic substituents with various electronic effects, allowing the formation of the amide linker. After an optimized amidination step, IC_{50} values of these compounds against FXIIa could be evaluated with the aim of assessing potency and selectivity by using other coagulation enzymes. Furthermore, aPTT and PT assays would be essential to evaluate their anticoagulant profile to ensure inhibition only affects the intrinsic pathway of coagulation.

A different approach could be considered to avoid complications associated with the nitrile group, which could interfere with sensitive steps: this alternative strategy could involve the use of dihalogenated aryl compounds, such as 1,4-dibromobenzene or 1-bromo-4-iodobenzene. Malonate cross-coupling reactions could be performed according to the effective protocol established, followed by reduction using stronger reducing agents to access the diol without the risk of nitrile reduction. The synthesis could then proceed as described, and the nitrile group would only be introduced at a late stage *via* a cyanation coupling, significantly reducing the problems encountered and associated with the nitrile group.

In a longer-term perspective, once optimized FXIIa inhibitors are obtained, further structural optimization could be envisioned to improve their drug-like properties: replacing the amide linker with a suitable bioisostere such as oxetane, as well as varying the linker length could optimize interactions with FXIIa while improving compatibility with oral administration. The most promising compounds would then require *in vivo* pharmacokinetic evaluation, with a focus on oral bioavailability, in order to assess their potential as a clinical medication to prevent the bleeding risk associated with current anticoagulants.

EXPERIMENTAL SECTION

1. INSTRUMENTATION

1.1. ^{1}H NMR spectroscopy

^{1}H NMR spectra were acquired on a JEOL JMTC-400 with a frequency of 400 MHz, or JNM ECZ-500 with a frequency of 500 MHz. Samples were prepared in 5 mm borosilicate tubes at room temperature in deuterated solvents. Peak resolutions are achieved using the Delta program. Chemical shifts (δ) are reported in ppm and calibrated using the residual solvent signals as an internal reference ($CDCl_3$ δH = 7.26 ppm ; $(CD_3)_2SO$ δH = 2.50 ppm ; D_2O δH = 4.79 ppm). Coupling constants (J) are reported in Hertz (Hz). The resonance multiplicity is described as s (singlet), d (doublet), t (triplet), q (quartet), qn (quintet), m (multiplet).

1.2. ^{13}C NMR spectroscopy

^{13}C NMR spectra were acquired on a JEOL JNM ECZ-500 with a frequency of 125 MHz. Samples were prepared in 5 mm quartz tubes at room temperature in deuterated solvents. Peak resolutions are achieved using the Delta program. Chemical shifts (δ) are reported in ppm and calibrated using the residual solvent signals as an internal reference ($CDCl_3$ δC = 77.16 ppm ; $(CD_3)_2SO$ δC = 39.52 ppm).

1.3. ^{19}F NMR spectroscopy

^{19}F NMR spectra were acquired on a JEOL JNM ECZ-500 with a frequency of 470 MHz. Samples were prepared in 5 mm quartz tubes at room temperature in deuterated solvents. Peak resolutions are achieved using the Delta program. Chemical shifts (δ) are reported in ppm.

1.4. Infrared spectroscopy

IR spectra were acquired on a Perkin-Elmer Spectrum Two FT-IR System UATR. The spectra were measured between wavenumbers of 500-4000 cm^{-1}.

1.5. Melting point

M_p were measured in a Büchi Melting Point M-560 in open capillaries.

1.6. High resolution mass spectrometry

HRMS analyses were acquired on a Bruker MaXis Impact Q-TOF spectrometer by the MaSUN platform of University of Namur. Samples were diluted in adequate solvents with a concentration of 1 mg/mL and diluted 500 times in a H_2O/MeCN (1:1) mixture. Diluted solutions (200 µL) are

sent in the ESI source by a Harvard syringe pump with a flow of 180 µL/min. ESI conditions are as follows: capillary voltage is set at 4.5 kV, dry nitrogen is used as a nebulizer gas at 0.4 bar and as a drying gas at 180°C. ESI spectra are acquired at 1 Hz in a 50-300 m/z range. Calibration was performed with an ESI-TOF reference mixture from Agilent. Data are processed by Bruker DataAnalysis 4.1 software.

1.7. X-ray diffraction

Solid-state XRD data were acquired using an Oxford Diffraction Gemini R Ultra diffractometer with copper Kα radiation (λ = 1,54 Å) at 295 K. Data analysis and crystal lattice determination were performed using CrysAlis PRO software. Graphical representation of the single crystals was performed using Mercury software.

1.8. Thin layer chromatography

TLC were performed using Merck aluminum silica gel 60 F_{254} TLC plates and monitored by UV light at 254 nm or $KMnO_4$ solution (3 g $KMnO_4$, 20 g K_2CO_3, and 5 mL aqueous NaOH 5% in 300 mL distilled water). Retention factor (R_f) was calculated by dividing the distance of the product on the TLC plate by the distance of the elution front.

1.9. Column chromatography

Column chromatography purifications were performed under pressure using Carl Roth silica gel 60 (40-63 µm). Prepared eluants used technical grade solvents that were distilled beforehand. In some cases, the use of demetallated silica is required, which is prepared according to the following procedure: Carl Roth silica 60 is treated in a bath of 10% aqueous HCl and stirred every half hour for one day. The silica is then left to settle and the supernatant is removed. The silica is rinsed with distilled water, left to settle, and the supernatant is removed again. This rinsing cycle is repeated until the pH is neutral. The silica is then filtered and left to dry on filter paper.[94]

2. REAGENTS, SOLVENTS AND METHODS

Reagents and solvents were purchased from Acros, BLDPharm, Carbosynth, Fischer Scientific, Fluorochem, Merck, or TCI and used without further purification. Deuterated solvents ($CDCl_3$, $(CD_3)_2SO$, and D_2O) were purchased from Euriso-top.

Reactions performed under argon used dry solvents. Dry conditioning of the glassware was realized manually by heating the glassware with a heat gun under a flux of argon for 3 minutes.

Et_2O, THF, and toluene were dried over a Pure Solv solvent purification system. Degassed solvents were obtained using four freeze-pump-thaw cycles.

Baths for low-temperature experiments were prepared as followed: water/ice (0°C), MeCN/liquid N_2 (-46 to -35°C), acetone/dry ice (-78°C).

Evaporation and concentration under reduced pressure were performed at 50°C and compounds were dried at a maximum pressure of 10 mbar.

3. SYNTHETIC PROCEDURES

General procedure A, B and C: synthesis of aryl malonates

General procedure A. Protocol adapted from the literature.[78] A 25 mL round bottom flask under argon containing NaH (52 mg, 1.3 eq, 60% dispersion in mineral oil) and NMP (0.23 mL) was stirred at 0°C. To this flask was added dimethyl malonate (132 mg, 1.0 eq) in NMP (1 mL) dropwise over 30 minutes at 0°C. The resulting mixture was stirred at room temperature for 20 hours under argon to obtain sodium salt of dimethyl malonate in NMP. Another 25 mL round bottom flask under argon containing 4-cyanophenyl trifluoromethanesulfonate (**13a**) (250 mg, 1.0 eq), CuI (189 mg, 1.0 eq) and NMP (2 mL) was stirred at 80°C (reflux) for 1 hour. Sodium salt of dimethyl malonate was added at once to the CuI mixture obtained, NMP (0.5 mL) was added, and the reaction mixture was stirred at 100°C (reflux) for 71 hours. The crude mixture was poured on cold 1 M HCl (10 mL), AcOEt (20 mL) was added, and the mixture was stirred vigorously. The mixture was filtered on cotton, the filtrate was allowed to settle to obtain a biphasic mixture, and the layers were separated. The organic layer was washed with 50 mL distilled water and acidified with 1 M HCl until pH 4. The aqueous layer, to which 20 mL of brine were added, was extracted 2x with 50 mL AcOEt. The organic layers were combined, dried over Na_2SO_4, filtered and evaporated under reduced pressure. The residue was purified by column chromatography on silica gel eluting with 10:0 to 8:2/Cy:AcOEt.

General procedure B. Protocol adapted from the literature.[80] To a round bottom flask under argon, NaH (60% dispersion in mineral oil) was washed 3x with pentane and 1x with dry THF. To this flask were added dry THF, 4-cyanophenyl trifluoromethanesulfonate (**13a**) or 4-bromobenzonitrile (**13b**) (1.0 eq), dimethyl malonate (1.2 eq), $Pd(dba)_2$ (0.01 or 0.10 eq) and $P(t\text{Bu})_3HBF_4$ (0.02 or 0.20 eq). The reaction mixture was stirred at 70°C for several days under argon and monitored by TLC. The crude mixture was filtered through filter paper, and the solvent was evaporated under reduced pressure.

General procedure C. Protocol adapted from the literature.[81] To a round bottom flask under argon containing 4-cyanophenyl trifluoromethanesulfonate (**13a**) or 4-bromobenzonitrile (**13b**) (1.0 eq) in degassed dry toluene were added dimethyl malonate (1.1 eq), K_3PO_4 (3.0 eq), $Pd(OAc)_2$ (0.10 or 0.05 eq) and ligand (0.20 or 0.10 eq). The reaction mixture was stirred at 125°C for several hours under argon and monitored by TLC. The crude mixture was filtered through a plug of Celite and the solvent was evaporated under reduced pressure. The residue was purified by column chromatography on silica gel.

General procedure D: reduction with $LiBH_4$ in THF

Protocol adapted from the literature.[84–86] To a round bottom flask under argon containing dimethyl 2-(4-cyanophenyl)malonate (**14**) or dimethyl 2-(p-tolyl)malonate (**19**) (1.0 eq) were slowly added $LiBH_4$ powder, dry THF and MeOH (when specified) at 0°C. The reaction mixture was stirred at the specified temperature for several hours under argon and monitored by TLC. Distilled water was added, and the aqueous layer was extracted 3x with CH_2Cl_2. The organic layers were combined, dried over $MgSO_4$, filtered and evaporated under reduced pressure. The aqueous layer was retrieved, to which Rochelle tartrate solution and CH_2Cl_2 were added. The mixture was vigorously stirred for 30 minutes until the emulsion disappears to show a clear separation. The layers were separated, the aqueous layer was extracted 3x with CH_2Cl_2, the organic layers were combined, dried over $MgSO_4$, filtered and evaporated under reduced pressure.

General procedure E: reduction with $LiAlH_4$

Protocol adapted from the literature.[88] To a 25 mL round bottom flask under argon containing dimethyl 2-(4-cyanophenyl)malonate (**14**) (80 mg, 1.0 eq) were slowly added $LiAlH_4$ 2 M in THF (0.7 mL, 4.1 eq) and THF (3 mL) at 0°C. The reaction mixture was allowed to return to room temperature, stirred for 2.5 h under argon and monitored by TLC. 20 mL of aqueous NH_4Cl solution were added, and the layers were separated. The aqueous layer was extracted 3x with 50 mL AcOEt, the organic layers were combined, washed 2x with 150 mL distilled water, 1x with 150 mL brine, dried over Na_2SO_4, filtered and evaporated under reduced pressure.

General procedure F: reduction with DIBAL-H

Protocol adapted from the literature.[89] To a 50 mL round bottom flask under argon containing dimethyl 2-(4-cyanophenyl)malonate (**14**) (150 mg, 1.0 eq) were slowly added dry toluene (6 mL) and DIBAL-H 1 M in hexane (2.6 mL, 4.0 eq) at -78°C. The reaction mixture was stirred at -78°C for 3 h under argon and monitored by TLC. 3 mL of distilled water, 7 mL of Rochelle

tartrate solution and 20 mL of AcOEt were added and the mixture was vigorously stirred for 15 minutes until the emulsion disappears to show a clear separation. The layers were separated, the aqueous layer was extracted 2x with 30 mL AcOEt, the organic layers were combined, dried over Na_2SO_4, filtered and evaporated under reduced pressure.

General procedure G: reduction with $NaBH_4$ in MeOH

Protocol adapted from the literature.[90] To a 25 mL round bottom flask containing dimethyl 2-(4-cyanophenyl)malonate (**14**) (1.0 eq) were slowly added MeOH and $NaBH_4$ powder (6.1 eq) at 0°C. The reaction mixture was stirred at room temperature overnight and monitored by TLC. After completion of the reaction, the solvent was evaporated under reduced pressure, then distilled water and HCl 1 M were added until pH 7. The aqueous layer was extracted 4x with CH_2Cl_2, the organic layers were combined, dried over Na_2SO_4, filtered and evaporated under reduced pressure.

General procedure H: reduction with $NaBH_4$ in H_2O:dioxane (1:1)

Protocol adapted from the literature.[91] To a 25 mL round bottom flask containing dimethyl 2-(4-cyanophenyl)malonate (**14**) (1.0 eq) were slowly added H_2O:dioxane/1:1 and $NaBH_4$ powder (8.1 eq) at 0°C. The reaction mixture was stirred at room temperature overnight and monitored by TLC. After completion of the reaction, HCl 1 M was added until pH 7. The aqueous solution was extracted 3x with AcOEt, the organic layers were combined, dried over $MgSO_4$, filtered and evaporated under reduced pressure.

4-cyanophenyl trifluoromethanesulfonate (13a)

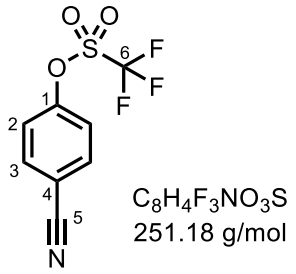

$C_8H_4F_3NO_3S$
251.18 g/mol

Protocol adapted from the literature.[77] To a 100 mL round bottom flask under argon containing 4-hydroxybenzonitrile (**17**) (1.811 g, 1.0 eq) in dry CH_2Cl_2 (15 mL) were slowly added 2,6-lutidine (4.2 mL, 2.4 eq) and trifluoromethanesulfonic anhydride (2.2 mL, 0.9 eq) at -35°C. The reaction mixture was stirred at room temperature for 6 h under argon and monitored by TLC. After completion of the reaction, 50 mL of distilled water were added. The layers were separated, the aqueous layer was extracted 3x with 30 mL CH_2Cl_2 and the organic layers were combined. The organic layers were washed 1x with 100 mL NaOH 2 M, 1x with 200 mL HCl 1 M, 1x with 100 mL brine, and dried over $MgSO_4$. The mixture was filtered and evaporated under reduced pressure. The residue was purified by column chromatography on silica gel eluting with 95:5/Cy:AcOEt to yield the desired product **13a** (3.013 g).

Aspect: Yellow oil

Yield: 99%

TLC: R_f = 0.33 (9:1/Cy:AcOEt), revealed by UV and $KMnO_4$

^{1}H NMR ($CDCl_3$, 500 MHz): δ (ppm) **7.79** (m, 2 H, J = 8.9 ; 2.6 Hz, C^2H), **7.43** (m, 2 H, J = 8.9 ; 2.6 Hz, C^3H)

^{13}C NMR ($CDCl_3$, 125 MHz): δ (ppm) **152.08** (C^1), **134.64** (C^3), **122.76** (C^2), **118,74** (q, J = 320.9 Hz, C^6), **117.23** (C^5), **113.02** (C^4)

^{19}F NMR ($CDCl_3$, 470 MHz): δ (ppm) **-72.50** (C^6F_3)

IR: $\bar{\nu}$ (cm^{-1}) **3110** (C^{Ar}–H), **2236** (C≡N), **1600** (C^{Ar}=C^{Ar}), **1426** (S=O), **1290** (CF_3), **1208** (S=O), **1136** (CF_3), **1020** (S=O), **846** (C^{Ar}–H)

HRMS: m/z calculated for $[M+Na]^+$ 273.9756, found 273.9752

Dimethyl 2-(4-cyanophenyl)malonate (14)

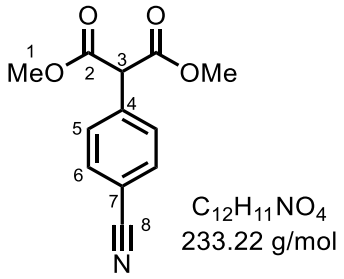

4-cyanophenyl trifluoromethanesulfonate (**13a**) or 4-bromobenzonitrile (**13b**) reacted according to general procedure C. The best results in the shortest time were obtained in entry 4 of Table 2, with 250 mg of **13a**. The residue was purified by column chromatography on silica gel eluting with 100:0 to 92:8/Cy:AcOEt to yield the desired product **14** (262 mg).

Aspect: White to light orange crystalline solid

Yield: 82%

TLC: R_f = 0.37 (7:3/Cy:AcOEt), revealed by UV and $KMnO_4$

M_p: 101°C

^{1}H NMR ($CDCl_3$, 500 MHz): δ (ppm) **7.67** (A portion of AB, 2 H, $\Delta\nu_{AB}$ = 65.5 Hz, J_{AB} = 8.0 Hz, C^6H), **7.54** (B portion of AB, 2 H, $\Delta\nu_{AB}$ = 65.5 Hz, J_{AB} = 8.0 Hz, C^5H), **4.70** (s, 1 H, C^3H), **3.77** (s, 6 H, C^1H_3)

^{13}C NMR ($CDCl_3$, 125 MHz): δ (ppm) **167.66** (C^2), **137.61** (C^4), **132.52** (C^6), **130.37** (C^5), **118.52** (C^8), **112.60** (C^7), **57.49** (C^3), **53.37** (C^1)

IR: $\bar{\nu}$ (cm^{-1}) **2961** (CH_3), **2230** (C≡N), **1726** (C=O), **1607** (C^{Ar}=C^{Ar}), **1433** (CH_3), **1149** (C–O), **843** (C^{Ar}–H)

HRMS: m/z calculated for $[M+Na]^+$ 256.0580, found 256.0581

4-(1,3-dihydroxypropan-2-yl)benzonitrile (15)

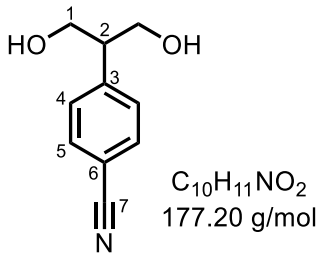

Dimethyl 2-(4-cyanophenyl)malonate (**14**) reacted according to general procedure G. The best results were obtained with 150 mg of **14**. The residue was purified by column chromatography on demetallated silica gel eluting with 10:0 to 0:10/Cy:AcOEt to yield the desired product **15** (33 mg).

Aspect: Light orange wax

Yield: 29%

Dimethyl 2-(4-cyanophenyl)malonate (**14**) reacted according to general procedure H. The best results were obtained with 200 mg of **14**. The residue was purified by column chromatography on demetallated silica gel eluting with 10:0 to 0:10/Cy:AcOEt to yield the desired product **15** (23 mg).

Aspect: Light orange wax

Yield: 15%

TLC: R_f = 0.29 (0:10/Cy:AcOEt), revealed by UV and $KMnO_4$

M_p: 82°C

^{1}H NMR ($CDCl_3$, 500 MHz): δ (ppm) **7.60** (A portion of AB, 2 H, $\Delta\nu_{AB}$ = 114.2 Hz, J_{AB} = 8.5 Hz, C^5H), **7.37** (B portion of AB, 2 H, $\Delta\nu_{AB}$ = 114.2 Hz, J_{AB} = 8.5 Hz, C^4H), **6.25** (X portion of ABX, J_{AX} = 26.2 Hz, J_{BX} = -14.2 Hz), **3.95** (A portion of ABX, 2 H, $\Delta\nu_{AB}$ = 12.1 Hz, J_{AB} = 11.0 Hz, J_{AX} = 26.2 Hz, C^1H_2), **3.94** (B portion of ABX, 2 H, $\Delta\nu_{AB}$ = 12.1 Hz, J_{AB} = 11.0 Hz, J_{BX} = -14.2 Hz, C^1H_2), **3.10** (qn, 1 H, J = 5.6 Hz, C^2H)

^{13}C NMR ($CDCl_3$, 125 MHz): δ (ppm) **145.71** (C^3), **132.51** (C^5), **129.12** (C^4), **118.87** (C^7), **110.86** (C^6), **65.00** (C^1), **49.59** (C^2)

IR: $\bar{\nu}$ (cm^{-1}) **3467** (O–H), **2923** (CH_2), **2884** (CH), **2237** (C≡N), **1609** (C^{Ar}=C^{Ar}), **1468** (CH_2), **1419** (O–H), **1121** (C–O), **835** (C^{Ar}–H)

HRMS: m/z calculated for $[M+Na]^+$ 200.0682, found 200.0680

Amino(4-(1,3-dihydroxypropan-2-yl)phenyl)methaniminium chloride (16b)

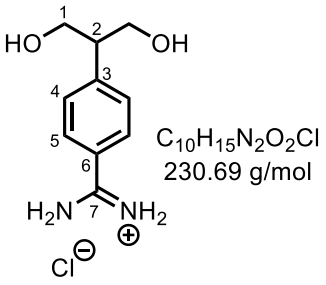

Protocol adapted from a previous researcher's[76] and the literature.[92] To a 25 mL round bottom flask under argon containing 4-(1,3-dihydroxypropan-2-yl)benzonitrile (**15**) (101 mg, 1.0 eq) in dry THF (1.2 mL) was slowly added LiHMDS 1 M in THF (1.4 mL, 2.5 eq) at 0°C. The reaction mixture was stirred at 60°C (reflux) for 5 h under argon and monitored by TLC. After completion of the reaction, the solution was cooled down to 0°C to which was slowly added 0.5 mL of HCl 37%. The yellow liquid was separated from the white precipitate, and the precipitate was evaporated under reduced pressure. The obtained paste was put in the oven at 100°C for an hour to yield the desired product **16b**.

Aspect: Beige solid paste

M_p: 270°C (decomposition)

^{1}H NMR (D_2O, 400 MHz): δ (ppm) **7.72** (A portion of AB, 2 H, $\Delta\nu_{AB}$ = 109.7 Hz, J_{AB} = 8.0 Hz, C^5H), **7.45** (B portion of AB, 2 H, $\Delta\nu_{AB}$ = 109.7 Hz, J_{AB} = 8.0 Hz, C^4H), **3.85** (A portion of ABX, 2 H, $\Delta\nu_{AB}$ = 17.4 Hz, J_{AB} = 11.0 Hz, J_{AX} = 5.9 Hz, C^1H_2), **3.79** (B portion of ABX, 2 H, $\Delta\nu_{AB}$ = 17.4 Hz, J_{AB} = 11.0 Hz, J_{BX} = 8.1 Hz, C^1H_2), **3.13** (qn, 1 H, C^2H)

^{13}C NMR (D_2O, 125 MHz): δ (ppm) **146.29** (C^3), **132.66** (C^5), **129.22** (C^4), **109.57** (C^6), **62.51** (C^1), **50.15** (C^2)

IR: $\bar{\nu}$ (cm^{-1}) **3118** (O–H and N–H), **2805** (CH_2), **1751** (C=N), **1394** (C–N), **837** (C^{Ar}–H)

HRMS: m/z calculated for $[M]^+$ 195.1128, found 195.1124

Dimethyl 2-(p-tolyl)malonate (19)

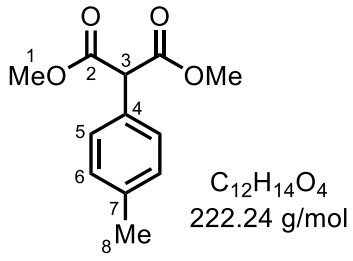

1-bromo-4-methylbenzene (**18**) reacted according to general procedure C. The residue was purified by column chromatography on silica gel eluting with 100:0 to 97:3/Cy:AcOEt to yield the desired product **19** (43 mg).

Aspect: Yellow-orange waxy oil

Yield: 13%

TLC: R_f = 0.38 (8:2/Cy:AcOEt), revealed by UV and $KMnO_4$

M_p: 68-70°C[95]

^{1}H NMR ($CDCl_3$, 400 MHz): δ (ppm) **7.27** (A portion of AB, 2 H, $\Delta\nu_{AB}$ = 40.4 Hz, J_{AB} = 7.0 Hz, C^5H), **7.17** (B portion of AB, 2 H, $\Delta\nu_{AB}$ = 40.4 Hz, J_{AB} = 7.0 Hz, C^6H), **4.61** (s, 1 H, C^3H), **3.74** (s, 6 H, C^1H_3), **2.34** (s, 3 H, C^8H_3)

^{13}C NMR ($CDCl_3$, 125 MHz): δ (ppm) **168.60** (C^2), **138.10** (C^7), **129.53** (C^4), **129.33** (C^5), **129.00** (C^6), **57.14** (C^3), **52.74** (C^1), **21.06** (C^8)

No **HRMS** nor **IR** analyses have been conducted.

4-(2-hydroxyethyl)benzonitrile (20)

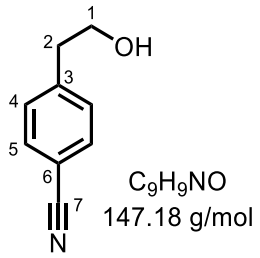

Dimethyl 2-(4-cyanophenyl)malonate (**14**) reacted according to general procedure G. The best results were obtained with 150 mg of **14**. The residue was purified by column chromatography on silica gel eluting with 10:0 to 0:10/Cy:AcOEt to yield the desired product **20** (48 mg).

Aspect: Light orange wax

Yield: 50%

Dimethyl 2-(4-cyanophenyl)malonate (**14**) reacted according to general procedure H. The best results were obtained with 200 mg of **14**. The residue was purified by column chromatography on silica gel eluting with 10:0 to 0:10/Cy:AcOEt to yield the desired product **20** (44 mg).

Aspect: Light orange wax

Yield: 45%

TLC: R_f = 0.48 (3:7/Cy:AcOEt), revealed by UV and $KMnO_4$

M_p: 50-51°C[96]

^{1}H NMR ($CDCl_3$, 500 MHz): δ (ppm) **7.56** (A portion of AB, 2 H, $\Delta\nu_{AB}$ = 115.6 Hz, J_{AB} = 9.0 Hz, C^5H), **7.33** (B portion of AB, 2 H, $\Delta\nu_{AB}$ = 115.6 Hz, J_{AB} = 9.0 Hz, C^4H), **3.85** (t, 2 H, J = 6.5 Hz, C^1H_2), **2.90** (t, 2 H, J = 6.4 Hz, C^2H_2)

^{13}C NMR ($CDCl_3$, 125 MHz): δ (ppm) **144.80** (C^3), **132.28** (C^5), **129.93** (C^4), **119.03** (C^7), **110.12** (C^6), **62.84** (C^1), **39.17** (C^2)

IR: $\bar{\nu}$ (cm^{-1}) **3425** (O–H), **2921** (CH_2), **2228** (C≡N), **1609** (C^{Ar}=C^{Ar}), **1457** (CH_2), **1178** (C–O), **824** (C^{Ar}–H)

HRMS: m/z calculated for $[M+Na]^+$ 170.0576, found 170.0575

4-(2-((tert-butyldimethylsilyl)oxy)ethyl)benzonitrile (23)

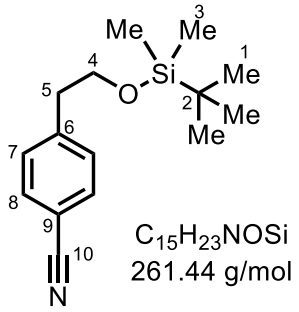

To a 25 mL round bottom flask under argon containing 4-(2-hydroxyethyl)benzonitrile (**20**) (91 mg, 1.0 eq) were added TBDMSCl (148 mg, 1.6 eq), imidazole (81 mg, 1.9 eq) and dry DMF (0.9 mL) at 0°C. The reaction mixture was stirred for 20 minutes at 0°C, then stirred at room temperature for 16.5 h under argon and monitored by TLC. After completion of the reaction, 10 mL of Et_2O were added, and the organic layer was washed 5x with 10 mL of a mixture of H_2O:brine/1:1. The organic layer was dried over $MgSO_4$, filtered and evaporated under reduced pressure.

Aspect: Yellow oil

Yield: 82%

TLC: R_f = 0.38 (92:8/Cy:AcOEt), revealed by UV and $KMnO_4$

^{1}H NMR ($CDCl_3$, 500 MHz): δ (ppm) **7.57** (A portion of AB, 2 H, $\Delta\nu_{AB}$ = 126.8 Hz, J_{AB} = 8.0 Hz, C^8H), **7.32** (B portion of AB, 2 H, $\Delta\nu_{AB}$ = 126.8 Hz, J_{AB} = 8.0 Hz, C^7H), **3.82** (t, 2 H, J = 6.4 Hz, C^4H_2), **2.86** (t, 2 H, J = 6.3 Hz, C^5H_2), **0.84** (s, 9 H, C^1H_3), **-0.06** (s, 6H, C^3H_3)

^{13}C NMR ($CDCl_3$, 125 MHz): δ (ppm) **145.44** (C^6), **132.07** (C^8), **130.17** (C^7), **119.29** (C^{10}), **110.05** (C^9), **63.60** (C^4), **39.64** (C^5), **25.94** (C^1), **18.38** (C^2), **-5.38** (C^3)

IR: $\bar{\nu}$ (cm^{-1}) **2953** (CH_3), **2928** (CH_2), **2228** (C≡N), **1609** (C^{Ar}=C^{Ar}), **1472** (CH_2), **1256** (Si–CH_3), **1095** (C–O), **831** (C^{Ar}–H), **776** (Si–CH_3)

HRMS: m/z calculated for $[M+Na]^+$ 284.1441, found 284.1439

Methyl 2-(4-cyanophenyl)acetate (26)

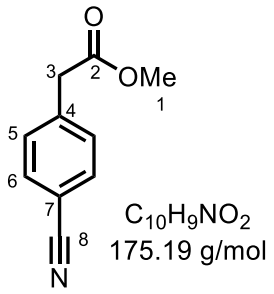

Protocol adapted from the literature.[93] To a 25 mL round bottom flask containing dimethyl 2-(4-cyanophenyl)malonate (**14**) (300 mg, 1.0 eq) were added LiCl (366 mg, 6.5 eq), DMSO (3 mL) and distilled water (1 mL). The reaction mixture was stirred at 100°C (reflux) for 17 h and monitored by TLC. After completion of the reaction, 40 mL of distilled water were added, and the aqueous layer was extracted 5x with 50 mL AcOEt. The organic layers were washed 5x with 200 mL H_2O:brine/1:1, dried over Na_2SO_4, filtered and evaporated under reduced pressure. The residue was purified by column chromatography on silica gel eluting with 10:0 to 7:3/Cy:TBME to yield the desired product **26** (109 mg).

Aspect: Light yellow oil

Yield: 48%

TLC: R_f = 0.50 (5:5/Cy:TBME), revealed by UV and $KMnO_4$

^{1}H NMR ($CDCl_3$, 400 MHz): δ (ppm) **7.62** (A portion of AB, 2 H, $\Delta\nu_{AB}$ = 89.6 Hz, J_{AB} = 8.0 Hz, C^6H), **7.39** (B portion of AB, 2 H, $\Delta\nu_{AB}$ = 89.6 Hz, J_{AB} = 8.0 Hz, C^5H), **3.71** (s, 3 H, C^1H_3), **3.69** (s, 2 H, C^3H_2)

^{13}C NMR ($CDCl_3$, 125 MHz): δ (ppm) **170.88** (C^2), **139.33** (C^4), **132.45** (C^6), **130.29** (C^5), **118.81** (C^8), **111.29** (C^7), **52.48** (C^1), **41.16** (C^3)

IR: $\bar{\nu}$ (cm^{-1}) **3000** (C^{Ar}–H), **2957** (CH_3), **2919** (CH_2), **2227** (C≡N), **1726** (C=O), **1610** (C^{Ar}=C^{Ar}), **1456** (CH_3), **1441** (CH_2), **1171** (C–O), **826** (C^{Ar}–H)

HRMS: m/z calculated for $[M+H]^+$ 176.0706, found 176.0703

4. ADDITIONAL STRUCTURES

XRD and crystal structure of dimethyl 2-(4-cyanophenyl)malonate (14)

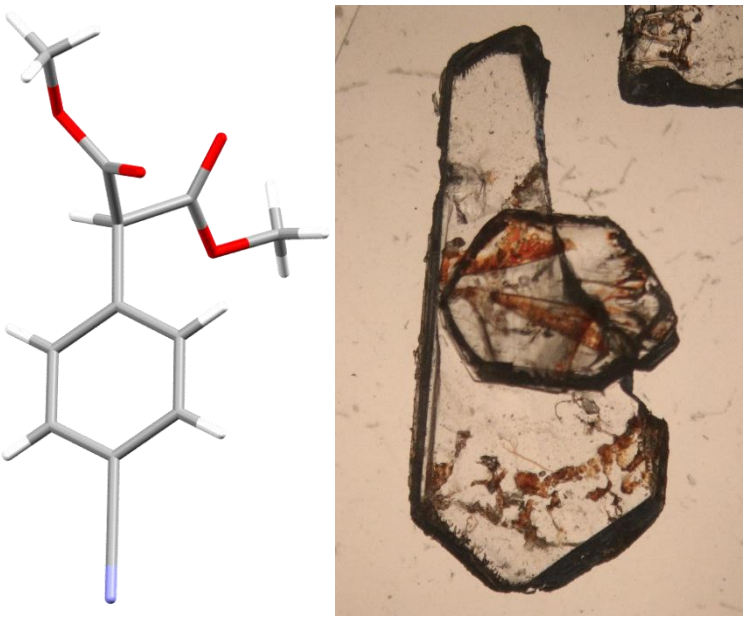

Buchwald's dialkylbiaryl phosphine ligands

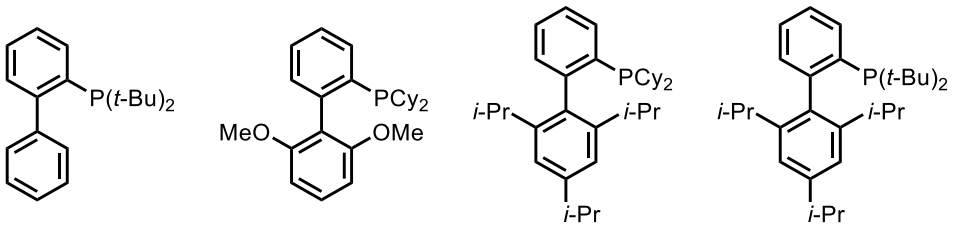

JohnPhos **SPhos** **XPhos** ***t*BuXPhos**

REFERENCES

(1) Van Hinsbergh, V. W. M. *Semin. Immunopathol.* **2012**, *34*, 93–106.

(2) Gale, A. J. *Toxicol. Pathol.* **2011**, *39*, 273–280.

(3) Hoffman, R. in *Hematology: Basic Principles and Practice*, 7th edition.; Elsevier: Philadelphia, PA, **2018**.

(4) Houdijk, W. P.; De Groot, P. G.; Nievelstein, P. F.; Sakariassen, K. S.; Sixma, J. J. *Arterioscler. Off. J. Am. Heart Assoc. Inc* **1986**, *6*, 24–33.

(5) Macfarlane, R. G. *Nature* **1964**, *202*, 498–499.

(6) Davie, E. W.; Ratnoff, O. D. *Science* **1964**, *145*, 1310–1312.

(7) Loscalzo, J., Fauci, A. S., Kasper, D. L., Hauser, S. L., Longo, D. L., Jameson, J. L. in *Harrison's Principles of Internal Medicine*, 21st edition.; McGraw Hill: New York, **2022**.

(8) Wendelboe, A. M.; Raskob, G. E. *Circ. Res.* **2016**, *118*, 1340–1347.

(9) Raskob, G. E.; Angchaisuksiri, P.; Blanco, A. N.; Buller, H.; Gallus, A.; Hunt, B. J.; Hylek, E. M.; Kakkar, A.; Konstantinides, S. V.; McCumber, M.; Ozaki, Y.; Wendelboe, A.; Weitz, J. I. *Arterioscler. Thromb. Vasc. Biol.* **2014**, *34*, 2363–2371.

(10) Koupenova, M.; Kehrel, B. E.; Corkrey, H. A.; Freedman, J. E. *Eur. Heart J.* **2017**, *38* (11), 785–791.

(11) Furie, B.; Furie, B. C. *N. Engl. J. Med.* **2008**, *359*, 938–949.

(12) Libby, P.; Buring, J. E.; Badimon, L.; Hansson, G. K.; Deanfield, J.; Bittencourt, M. S.; Tokgözoğlu, L.; Lewis, E. F. *Nat. Rev. Dis. Primer* **2019**, *5*, 56.

(13) Lamichhane, M.; Salehi, N.; Ahmadjee, A.; Abela, G. S. in *Cardiovascular Thrombus*; Elsevier, **2018**; pp 15–30.

(14) Virchow, R. in *Thrombosis and Embolie: 1846 - 1856*; Matzdorff, A. C., Bell, W. R., Translators; Science History Publ: Canton, Mass, **1998**.

(15) Mackman, N. *J. Clin. Invest.* **2012**, *122*, 2331–2336.

(16) Jaffer, I. H.; Fredenburgh, J. C.; Hirsh, J.; Weitz, J. I. *J. Thromb. Haemost.* **2015**, *13*, S72–S81.

(17) Heestermans, M.; Poenou, G.; Hamzeh-Cognasse, H.; Cognasse, F.; Bertoletti, L. *Cells* **2022**, *11*, 3214.

(18) Marchetti, M.; Zermatten, M. G.; Bertaggia Calderara, D.; Aliotta, A.; Alberio, L. *J. Clin. Med.* **2021**, *10*, 683.

(19) Caterina, R. D.; Husted, S.; Wallentin, L.; Andreotti, F.; Arnesen, H.; Bachmann, F.; Baigent, C.; Huber, K.; Jespersen, J.; Kristensen, S. D.; Lip, G. Y. H.; Morais, J.; Rasmussen, L. H.; Siegbahn, A.; Verheugt, F. W. A.; Weitz, J. I. *Thromb. Haemost.* **2013**, *110*, 1087–1107.

(20) Chen, A.; Stecker, E.; A. Warden, B. *J. Am. Heart Assoc.* **2020**, *9*, e017559.

(21) Ratnoff, O. D.; Colopy, J. E. *J. Clin. Invest.* **1955**, *34*, 602–613.

(22) Ratnoff, O. D.; Davie, E. W. *Biochemistry* **1962**, *1*, 967–975.

(23) Schmaier, A. H. *J. Clin. Invest.* **2008**, *118*, 3006–3009.

(24) Schmaier, A. H.; Stavrou, E. X. *Res. Pract. Thromb. Haemost.* **2019**, *3*, 599–606.

(25) Cochrane, C. G.; Revak, S. D.; Wuepper, K. D. *J. Exp. Med.* **1973**, *138*, 1564–1583.

(26) Kaplan, A. P.; Meier, H. L.; Mandle, R. J. *Semin. Thromb. Hemost.* **1976**, *3*, 1–26.

(27) Renné, T.; Pozgajová, M.; Grüner, S.; Schuh, K.; Pauer, H.-U.; Burfeind, P.; Gailani, D.; Nieswandt, B. *J. Exp. Med.* **2005**, *202*, 271–281.

(28) Stavrou, E.; Schmaier, A. H. *Thromb. Res.* **2010**, *125*, 210–215.

(29) Cool, D. E.; MacGillivray, R. T. *J. Biol. Chem.* **1987**, *262*, 13662–13673.

(30) Davoine, C.; Bouckaert, C.; Fillet, M.; Pochet, L. *Eur. J. Med. Chem.* **2020**, *208*, 112753.

(31) De Maat, S.; Tersteeg, C.; Herczenik, E.; Maas, C. *Int. J. Lab. Hematol.* **2014**, *36*, 374–381.

(32) Dementiev, A.; Silva, A.; Yee, C.; Li, Z.; Flavin, M. T.; Sham, H.; Partridge, J. R. *Blood Adv.* **2018**, *2*, 549–558.

(33) Renné, T.; Schmaier, A. H.; Nickel, K. F.; Blombäck, M.; Maas, C. *Blood* **2012**, *120*, 4296–4303.

(34) Kenne, E.; Renné, T. *Drug Discov. Today* **2014**, *19*, 1459–1464.

(35) Kenne, E.; Nickel, K. F.; Long, A. T.; Fuchs, T. A.; Stavrou, E. X.; Stahl, F. R.; Renné, T. *J. Intern. Med.* **2015**, *278*, 571–585.

(36) Naudin, C.; Burillo, E.; Blankenberg, S.; Butler, L.; Renné, T. *Semin. Thromb. Hemost.* **2017**, *43*, 814–826.

(37) Wu, Y. *Thromb. J.* **2015**, *13*, 17.

(38) Kuchinka, J.; Willems, C.; Telyshev, D. V.; Groth, T. *Bioengineering* **2021**, *8*, 215.

(39) Renné, T.; Schmaier, A. H.; Nickel, K. F.; Blombäck, M.; Maas, C. *Blood* **2012**, *120*, 4296–4303.

(40) Raghunathan, V.; Zilberman-Rudenko, J.; Olson, S. R.; Lupu, F.; McCarty, O. J. T.; Shatzel, J. J. *Res. Pract. Thromb. Haemost.* **2019**, *3*, 331–339.

(41) Schmaier, A. H.; Mccrae, K. R. *J. Thromb. Haemost.* **2007**, *5*, 2323–2329.

(42) Pixley, R. A.; De La Cadena, R.; Page, J. D.; Kaufman, N.; Wyshock, E. G.; Chang, A.; Taylor, F. B.; Colman, R. W. *J. Clin. Invest.* **1993**, *91*, 61–68.

(43) Jansen, P.; Pixley, R.; Brouwer, M.; De Jong, I.; Chang, A.; Hack, C.; Taylor, F. J.; Colman, R. *Blood* **1996**, *87*, 2337–2344.

(44) Zamolodchikov, D.; Chen, Z.-L.; Conti, B. A.; Renné, T.; Strickland, S. *Proc. Natl. Acad. Sci.* **2015**, *112*, 4068–4073.

(45) Zamolodchikov, D.; Renné, T.; Strickland, S. *J. Thromb. Haemost.* **2016**, *14*, 995–1007.

(46) Pauer, H.-U.; Renné, T.; Hemmerlein, B.; Legler, T.; Fritzlar, S.; Adham, I.; Müller-Esterl, W.; Emons, G.; Sancken, U.; Engel, W.; Burfeind, P. *Thromb. Haemost.* **2004**, *92*, 503–508.

(47) Cheng, Q.; Tucker, E. I.; Pine, M. S.; Sisler, I.; Matafonov, A.; Sun, M.; White-Adams, T. C.; Smith, S. A.; Hanson, S. R.; McCarty, O. J. T.; Renné, T.; Gruber, A.; Gailani, D. A *Blood* **2010**, *116*, 3981–3989.

(48) Kleinschnitz, C.; Stoll, G.; Bendszus, M.; Schuh, K.; Pauer, H.-U.; Burfeind, P.; Renné, C.; Gailani, D.; Nieswandt, B.; Renné, T.. *J. Exp. Med.* **2006**, *203*, 513–518.

(49) Yau, J. W.; Liao, P.; Fredenburgh, J. C.; Stafford, A. R.; Revenko, A. S.; Monia, B. P.; Weitz, J. I. *Blood* **2014**, *123*, 2102–2107.

(50) Larsson, M.; Rayzman, V.; Nolte, M. W.; Nickel, K. F.; Björkqvist, J.; Jämsä, A.; Hardy, M. P.; Fries, M.; Schmidbauer, S.; Hedenqvist, P.; Broomé, M.; Pragst, I.; Dickneite, G.; Wilson, M. J.; Nash, A. D.; Panousis, C.; Renné, T. *Sci. Transl. Med.* **2014**, *6*, 222ra17.

(51) Matafonov, A.; Leung, P. Y.; Gailani, A. E.; Grach, S. L.; Puy, C.; Cheng, Q.; Sun, M.; McCarty, O. J. T.; Tucker, E. I.; Kataoka, H.; Renné, T.; Morrissey, J. H.; Gruber, A.; Gailani, D. *Blood* **2014**, *123*, 1739–1746.

(52) Wallisch, M.; Lorentz, C. U.; Lakshmanan, H. H. S.; Johnson, J.; Carris, M. R.; Puy, C.; Gailani, D.; Hinds, M. T.; McCarty, O. J. T.; Gruber, A.; Tucker, E. I. *Res. Pract. Thromb. Haemost.* **2020**, *4*, 205–216.

(53) Halbmayer, W.-M.; Haushofer, A.; Schön, R.; Mannhalter, C.; Strohmer, E.; Baumgarten, K.; Fischer, M. *Thromb. Haemost.* **1994**, *71*, 068–072.

(54) Gordon, E. M.; Donaldson, V. H.; Saito, H.; Su, E.; Ratnoff, O. D. *Ann. Intern. Med.* **1981**, *95*, 697–700.

(55) Escobar, M. A. Less Common Congenital Disorders of Hemostasis in *Consultative Hemostasis and Thrombosis*; Elsevier, **2019**; pp 59–79.

(56) Cao, H.; Biondo, M.; Lioe, H.; Busfield, S.; Rayzman, V.; Nieswandt, B.; Bork, K.; Harrison, L. C.; Auyeung, P.; Farkas, H.; Csuka, D.; Pelzing, M.; Dower, S.; Wilson, M. J.; Nash, A.; Nolte, M. W.; Panousis, C. *J. Allergy Clin. Immunol.* **2018**, *142*, 1355–1358.

(57) A Phase 4 Open-Label Study to Evaluate the Safety After Switching to CSL312 (Garadacimab) From Current Prophylactic HAE Treatment in Subjects With HAE ≥ 12 Years of Age, **2025**. https://clinicaltrials.gov/study/NCT06806657 (accessed 2025-12-01).

(58) Hansson, K. M.; Nielsen, S.; Elg, M.; Deinum, J. *J. Thromb. Haemost.* **2014**, *12*, 1678–1686.

(59) Yau, J. W.; Stafford, A. R.; Liao, P.; Fredenburgh, J. C.; Roberts, R.; Brash, J. L.; Weitz, J. I. *Acta Biomater.* **2012**, *8*, 4092–4100.

(60) Campos, I. T. N.; Tanaka-Azevedo, A. M.; Tanaka, A. S. *FEBS Lett.* **2004**, *577*, 512–516.

(61) Hagedorn, I.; Schmidbauer, S.; Pleines, I.; Kleinschnitz, C.; Kronthaler, U.; Stoll, G.; Dickneite, G.; Nieswandt, B. *Circulation* **2010**, *121*, 1510–1517.

(62) Decrem, Y.; Rath, G.; Blasioli, V.; Cauchie, P.; Robert, S.; Beaufays, J.; Frère, J.-M.; Feron, O.; Dogné, J.-M.; Dessy, C.; Vanhamme, L.; Godfroid, E. *J. Exp. Med.* **2009**, *206*, 2381–2395.

(63) Prajapathi, S.; Pradhan, A.; Mohta, A.; Sethi, R. *Egypt. Heart J.* **2024**, *76*, 137.

(64) Korff, M.; Imberg, L.; Will, J. M.; Bückreiß, N.; Kalinina, S. A.; Wenzel, B. M.; Kastner, G. A.; Daniliuc, C. G.; Barth, M.; Ovsepyan, R. A.; Butov, K. R.; Humpf, H.-U.; Lehr, M.; Panteleev, M. A.; Poso, A.; Karst, U.; Steinmetzer, T.; Bendas, G.; Kalinin, D. V. *J. Med. Chem.* **2020**, *63*, 13159–13186.

(65) Middendorp, S. J.; Wilbs, J.; Quarroz, C.; Calzavarini, S.; Angelillo-Scherrer, A.; Heinis, C. *J. Med. Chem.* **2017**, *60*, 1151–1158.

(66) Chen, Z.; Luo, B.; Cai, T.-Q.; Thankappan, A.; Xu, Y.; Wu, W.; DiMuzio, J.; Lifsted, T.; DiPietro, M.; Disa, J.; Ng, B.; Leander, K.; Clark, S.; Hoos, L.; Zhou, Y.; Jochnowitz, N.; Jachec, C.; Szczerba, P.; Gindy, M. E.; Strapps, W.; Sepp-Lorenzino, L.; Seiffert, D. A.; Lubbers, L.; Tadin-Strapps, M. *Mol. Ther. - Nucleic Acids* **2015**, *4*, e224.

(67) Dana, H.; Chalbatani, G. M.; Mahmoodzadeh, H.; Karimloo, R.; Rezaiean, O.; Moradzadeh, A.; Mehmandoost, N.; Moazzen, F.; Mazraeh, A.; Marmari, V.; Ebrahimi, M.; Rashno, M. M.; Abadi, S. J.; Gharagouzlo, E. *Int. J. Biomed. Sci. IJBS* **2017**, *13*, 48–57.

(68) Liu, J.; Qin, J.; Borodovsky, A.; Racie, T.; Castoreno, A.; Schlegel, M.; Maier, M. A.; Zimmerman, T.; Fitzgerald, K.; Butler, J.; Akinc, A. *RNA* **2019**, *25*, 255–263.

(69) Lauffer, M. C.; Van Roon-Mom, W.; Aartsma-Rus, A.; N = 1 Collaborative. *Commun. Med.* **2024**, *4*, 6.

(70) Dhuri, K.; Bechtold, C.; Quijano, E.; Pham, H.; Gupta, A.; Vikram, A.; Bahal, R. *J. Clin. Med.* **2020**, *9*, 2004.

(71) Revenko, A. S.; Gao, D.; Crosby, J. R.; Bhattacharjee, G.; Zhao, C.; May, C.; Gailani, D.; Monia, B. P.; MacLeod, A. R. *Blood* **2011**, *118*, 5302–5311.

(72) Platte, S.; Korff, M.; Imberg, L.; Balicioglu, I.; Erbacher, C.; Will, J. M.; Daniliuc, C. G.; Karst, U.; Kalinin, D. V. *ChemMedChem* **2021**, *16*, 3672–3690.

(73) Imberg, L.; Platte, S.; Erbacher, C.; Daniliuc, C. G.; Kalinina, S. A.; Dörner, W.; Poso, A.; Karst, U.; Kalinin, D. V. *ACS Pharmacol. Transl. Sci.* **2022**, *5*, 1318–1347.

(74) Bouckaert, C.; Serra, S.; Rondelet, G.; Dolušić, E.; Wouters, J.; Dogné, J.-M.; Frédérick, R.; Pochet, L. *Eur. J. Med. Chem.* **2016**, *110*, 181–194.

(75) Davoine, C.; Traina, A.; Evrard, J.; Lanners, S.; Fillet, M.; Pochet, L. *Eur. J. Med. Chem.* **2023**, *259*.

(76) Simon, F. Design and Synthesis of Phenylguanidine-Based and Benzamidine-Based FXIIa Inhibitors, University of Namur, **2020**.

(77) Uchiyama, M.; Kobayashi, Y.; Furuyama, T.; Nakamura, S.; Kajihara, Y.; Miyoshi, T.; Sakamoto, T.; Kondo, Y.; Morokuma, K. *J. Am. Chem. Soc.* **2008**, *130*, 472–480.

(78) Karnik, A. V.; Khadilkar, S. V.; Kadam, A.; Khose, V. N.; Gawde, P. M.; Khot, S. C.; Pansare, T. T., **2019**, IN 201821016281.

(79) Beare, N. A.; Hartwig, J. F. *J. Org. Chem.* **2002**, *67*, 541–555.

(80) Semmes, J. G.; Bevans, S. L.; Mullins, C. H.; Shaughnessy, K. H. *Tetrahedron Lett.* **2015**, *56*, 3447–3450.

(81) Pintchovski, S.; Shrader, W. D. **2024**, WO 2024081653.

(82) Stepan, A. F.; Subramanyam, C.; Efremov, I. V.; Dutra, J. K.; O'Sullivan, T. J.; DiRico, K. J.; McDonald, W. S.; Won, A.; Dorff, P. H.; Nolan, C. E.; Becker, S. L.; Pustilnik, L. R.; Riddell, D. R.; Kauffman, G. W.; Kormos, B. L.; Zhang, L.; Lu, Y.; Capetta, S. H.; Green, M. E.; Karki, K.; Sibley, E.; Atchison, K. P.; Hallgren, A. J.; Oborski, C. E.; Robshaw, A. E.; Sneed, B.; O'Donnell, C. J. *J. Med. Chem.* **2012**, *55*, 3414–3424.

(83) Skoreński, M.; Milewska, A.; Pyrć, K.; Sieńczyk, M.; Oleksyszyn, J. *J. Enzyme Inhib. Med. Chem.* **2019**, *34*, 8–14.

(84) Boyd, S.; Davies, C. D. *Tetrahedron Lett.* **2014**, *55*, 4117–4119.

(85) Yamamoto, K.; Tamura, T.; Nakamura, R.; Hosoe, S.; Matsubara, M.; Nagata, K.; Kodaira, H.; Uemori, T.; Takahashi, Y.; Suzuki, M.; Saito, J.; Ueno, K.; Shuto, S. *Bioorg. Med. Chem.* **2019**, *27*, 115122.

(86) Tang, H.; Walsh, S. P.; Yan, Y.; De Jesus, R. K.; Shahripour, A.; Teumelsan, N.; Zhu, Y.; Ha, S.; Owens, K. A.; Thomas-Fowlkes, B. S.; Felix, J. P.; Liu, J.; Kohler, M.; Priest, B. T.; Bailey, T.; Brochu, R.; Alonso-Galicia, M.; Kaczorowski, G. J.; Roy, S.; Yang, L.; Mills, S. G.; Garcia, M. L.; Pasternak, A. *ACS Med. Chem. Lett.* **2012**, *3*, 367–372.

(87) Chen, J.; Chen, X.; Bois-Choussy, M.; Zhu, J. *J. Am. Chem. Soc.* **2006**, *128*, 87–89.

(88) Chen, Y.-F.; Wu, C.-H.; Chen, L.-H.; Lee, H.-W.; Lee, J.-C.; Yeh, T.-K.; Chang, J.-Y.; Chou, M.-C.; Wu, H.-L.; Lai, Y.-P.; Song, J.-S.; Yeh, K.-C.; Chen, C.-T.; Lee, C.-J.; Shia, K.-S.; Shen, M.-R. *J. Med. Chem.* **2022**, *65*, 4767–4782.

(89) Dhungana, R. K.; Granados, A.; Ciccone, V.; Martin, R. T.; Majhi, J.; Sharique, M.; Gutierrez, O.; Molander, G. A. *ACS Catal.* **2022**, *12*, 15750–15757.

(90) Prasanth, C. P.; Ebbin, J.; Abhijith, A.; Nair, D. S.; Ibrahim, I.; Jevgenij, R.; Bakthan, S. *J. Org. Chem.* **2018**, *83*, 1431–1440.

(91) Bianco, A.; Passacantilli, P.; Righi, G. *Synth. Commun.* **1988**, *18*, 1765–1771.

(92) Boeré, R. T.; Oakley, R. T.; Reed, R. W. *J. Organomet. Chem.* **1987**, *331*, 161–167.

(93) Ates, A.; Jnoff, E.; Provins, L.; Valade, A.; Hall, A., **2017**, WO 2017178377.

(94) Hubbard, J. S.; Harris, T. M. *J. Org. Chem.* **1981**, *46*, 2566–2570.

(95) McLarney, B. D.; Hanna, S.; Musaev, D. G.; France, S. *ACS Catal.* **2019**, *9*, 4526–4538.

(96) Wagner, G.; Vieweg, H. *Pharmazie* **1982**, *37*, 13–16.